Available online at www.sciencedirect.com
ScienceDirect
Coordination Chemistry Reviews 251 (2007) 1834–1851
COORDINATION CHEMISTRY REVIEWS
www.elsevier.com/locate/ccr

Review

From nucleotides to ribozymes—A comparison of their metal ion binding properties☆

Eva Freisinger, Roland K.O. Sigel*

Institute of Inorganic Chemistry, University of Zürich, Winterthurerstrasse 190, CH-8057 Zürich, Switzerland

Received 15 January 2007; accepted 10 March 2007
Available online 20 March 2007

Contents

1. Introduction 1835
2. Control of reaction rates by metal ions in DNAzymes and ribozymes 1836
3. Metal ion binding to the building blocks of RNA and DNA 1837
   3.1. Metal ion binding to mononucleotides 1837
      3.1.1. Comments on the structure and function of nucleotides in solution 1837
      3.1.2. Stability of metal ion–nucleotide complexes in solution 1838
      3.1.3. Insights from crystallography 1840
   3.2. Metal ion binding to dinucleotides 1841
   3.3. The effect of structural preorientation in dinucleotides on metal ion binding 1843
4. Metal ion binding to ribozymes and DNA 1844
   4.1. Mg^{2+} binding to the ribosome 1845
   4.2. Metal ion binding to the HIV dimerization initiation site 1847
   4.3. Metal ion binding to the Dickerson–Drew DNA dodecamer 1848
5. Conclusions and outlook 1849
   Acknowledgements 1849
   References 1849

Abstract

It is undisputable that the fates of metal ions and nucleic acids are inescapably interwoven. Metal ions are essential for charge compensation of the negatively charged phosphate–sugar backbone, they are instrumental for proper folding, and last but not least they are crucial cofactors for ribozyme catalysis. Considerable progress has been achieved in the past few years on the identification of metal ion binding sites in large DNA and RNA molecules, like in ribozymes including the ribosome. Hereby, most information was gained from crystallography, which fails to explain metal ion binding equilibria in solution as well as the factors that determine the coordination of a metal ion to a specific site. In contrast, such information is readily available for the low-molecular building blocks of large nucleic acids, i.e. for mononucleotides and to some extent also dinucleotides. In this review, we combine and compare for the first time both sets of information. The focus is thereby set on Mg^{2+}, Ca^{2+}, Mn^{2+}, and Cd^{2+} because these four metal ions are either freely available in cells, have a large impact on the catalytic rate of ribozymes, and/or are often applied in RNA biochemistry. Our comparisons show that results obtained from small molecules can be directly transposed to the findings in large RNA structures like the ribosome. For example, the basic coordination-chemical properties of the different metal ions are reflected in their binding to large nucleic

Abbreviations: ADP^{3-}, adenosine 5′-diphosphate; A-form helix, regular RNA duplex with the ribose in its 2′-endo (*S*) configuration; AMP^{2-}, adenosine 5′-monophosphate; ATP^{4-}, adenosine 5′-triphosphate; CN, coordination number; cyt, cytosine; d, 2′-deoxy; $d(GpG)^{-}$, 2′-deoxyguanylyl(3′ → 5′)-2′-deoxyguanosine; $d(pGpG)^{3-}$, 2′-deoxyguanylyl(5′ → 3′)-2′-deoxy-5′-guanylate; $dGMP^{2-}$, 2′-deoxyguanosine 5′-monophosphate; $dNTP^{4-}$, 2′-deoxynucleoside 5′-triphosphate; GDP^{3-}, guanosine 5′-diphosphate; GMP^{2-}, guanosine 5′-monophosphate; GTP^{4-}, guanosine 5′-triphosphate; gua, guanine; *I*, ionic strength; K_a, acidity constant; NDP^{3-}, nucleoside 5′-diphosphate; NMP^{2-}, nucleoside 5′-monophosphate; NTP^{4-}, nucleoside 5′-triphosphate; NXP^{y-}, denotes the mono-, di-, or triphosphate form of any NMP^{2-}, NDP^{3-}, or NTP^{4-}; $pUpU^{3-}$, uridylyl(5′ → 3′)-5′-uridylate; thy, thymine; ura, uracil

☆ Based on a keynote lecture presented at the 37th International Conference on Coordination Chemistry, 13–18 August 2006, Cape Town, South Africa.

* Corresponding author. Tel.: +41 44 635 4652; fax: +41 44 635 6802.
E-mail address: roland.sigel@aci.uzh.ch (R.K.O. Sigel).

0010-8545/$ – see front matter
doi:10.1016/j.ccr.2007.03.008

acid structures: macrochelate formation, e.g. the simultaneous intranucleotide coordination of a Mg^{2+} ion to the phosphate unit and the N7 site of a purine nucleobase (be it inner- or outersphere), is well known for mononucleotides. We show that the frequency of occurrence of this type of coordination is the same for mononucleotides and the ribosome.

Keywords: Nucleic acids; Mono- and dinucleotides; Metal ions; RNA/DNA; Ribozymes

1. Introduction

Any RNA or nucleic acid is a polyanion due to the negatively charged phosphate–sugar backbone. Nevertheless, large RNAs fold to very complex three-dimensional structures containing not only A-form helices but also loops, bulges, and many other local structures, which form a multitude of tertiary contacts [1–4]. Consequently, negative charges accumulate in close space and need to be neutralized site-specifically in order to enable such close packing of the backbones. This is only achievable by positive charges of high density, i.e. metal ions [5–8]. The major task of charge compensation along the backbone is certainly taken over by monovalent ions (Na^+, K^+) [9], loosely bound divalent metal ions [10–14], and to some extent also by polycharged organic cations like spermine [7,15–18]. However, it is evident that divalent metal ions are the major source of specifically and locally bound positive charges within nucleic acids or living cells in general [7,8,19–22].

Among the divalent metal ions, Mg^{2+} is certainly the most abundant one being freely available in any cell and thus thought to be involved predominantly with RNA folding and catalysis [7,8,23–26]. Unfortunately, in terms of experimental detectability, Mg^{2+} is a nuisance because it offers no direct spectroscopic handle for detection, and its equal number of electrons makes it difficult to distinguish from H_2O or Na^+ in crystal structures [27]: high resolution is needed to identify Mg^{2+} ions in large nucleic acid structures, but most often such high resolution is not reached. In addition, to make the situation more complicated, one is interested only in a handful of Mg^{2+} ions bound at specific sites—but these are located within a vast sea of more loosely bound ions of the same kind around the RNA [21]. Among the specific sites only very few offer such a high affinity that they are saturated before others are filled up [7,21,28], e.g. triphosphate groups [29–32], positions within a pseudoknot [33,34], or a tetraloop–tetraloop receptor motif [35]. One possibility to monitor and investigate simultaneously metal ion binding to different sites including the characterization of the individual binding affinities is offered by Mg^{2+} titration experiments using NMR spectroscopy [29–31,36]. However, in most cases, as a consequence of the above-mentioned limitations, experimental strategies are followed by employing other metal ions than Mg^{2+}. To name just a few examples: (i) heavy atom derivatives for phasing in X-ray crystallography, (ii) lanthanide(III) ions [20,21,28], Pb^{2+} or transition metal ions [37,38] in hydrolytic cleavage experiments, (iii) lanthanide(III) ions in activity assays to elucidate the mechanism of ribozyme reactions [28], (iv) paramagnetic metal ions for EPR [39,40], and (v) the application of d^{10} or transition metal ions in NMR spectroscopy [29,41–43]. Many of such experiments have provided very valuable information on the location and role of distinct metal ions. However, the results are always associated with the caveat that another metal ion than the (presumably) native Mg^{2+} has been used—and it is evident from uncountable articles that every ion has its distinctive coordination chemistry.

As mentioned above, Mg^{2+} is certainly *the* divalent metal ion to be involved predominantly with RNA. However, it is dangerous to neglect all other metal ions with respect to RNA in natural systems, simply on the basis that they are not freely available in large quantities in every cell: most metalloproteins function on the basis of (redox active) metal ions that are highly toxic if freely available. These enzymes are thus chaperoned and loaded specifically with such ions [44]. Why should a similar mechanism not exist for RNA? In fact, there is growing evidence that other metal ions than Mg^{2+} can accelerate ribozyme reactions by manifolds, e.g. in the case of the hammerhead ribozyme [45–47]. In addition, there are several examples of both naturally occurring and *in vitro* designed ribozymes and DNAzymes [8,48–52], which show a fast decrease in reaction kinetics if trace amounts of other metal ions are present aside from the inherent one. It is therefore evident that not only Mg^{2+} but other metal ions as well need to be considered in order to understand the structure and function of nucleic acids in general, and of ribozymes specifically.

Summarizing the paragraphs above, a huge amount of information on M^{n+} binding to RNAs and their role in several catalytic mechanisms could be gained over the past years... with the already mentioned reservations: no other metal ion behaves absolutely identical to Mg^{2+} in terms of binding strength, coordination preferences, or simply size. It is therefore well feasible that incorrect conclusions regarding Mg^{2+} have been drawn in the past and misleading paths were followed when results obtained for Mg^{2+}-mimicking metal ions where prematurely assigned to Mg^{2+} itself. In order to interpret and validate the richness of data gained from such mimicking experiments and/or to discover and understand alternative metabolic pathways involving nucleic acids and metal ions, more and better information needs to be collected. Ideally an accurate knowledge of the distinct binding properties and preferences of each metal ion towards RNA or nucleic acids in general is highly desirable.

Such accurate data are scarce for larger nucleic acids, but small molecules like nucleobases, nucleosides, mono- or dinucleotides have been examined rigorously over the past years. Thereby, a richness of very accurate binding data for the most common metal ions to the building blocks of nucleic acids has accumulated. In this review, we combine for the first time this wealth of information existing on the binding properties of Mg^{2+}, Ca^{2+}, Mn^{2+}, and Cd^{2+} to mononucleotides and to dinucleotides in order to compare this information directly with what

Table 1
Comparison of some physico-chemical properties of Mg^{2+}, Ca^{2+}, Mn^{2+}, and Cd^{2+} in aqueous solution[a]

	Mg^{2+}	Ca^{2+}	Mn^{2+}	Cd^{2+}	References
Ionic radius (Å)	0.72	1.00 (1.12)[b]	0.83[c]	0.95	[170]
CN	6	6 (8)[b]	6	6	
Preferred ligands	O	O	O/N	N/O	
ΔH_{Hydr} (kJ mol^{-1})	1858	1570 (1657)[b]	1762	1640	[171]
M···OH_2 (Å)	2.04	2.37 (2.48)[b]	2.18	2.35	[171]
$pK^{H}_{M(H_2O)_6}$ (25 °C)	11.44 ± 0.1	12.85 ± 0.1	10.59	10.2	[172]
k_{exch} (s^{-1})	6.7×10^5	$\approx 10^9$	2.1×10^7	6.8×10^8	[173–175]

[a] Given are the ionic radii and the preferred coordination numbers (CN) of the M^{2+} ions, the enthalpies of hydration (ΔH_{Hydr}), the distances between the metal ion and a coordinated water molecule, the acidity constants ($pK^{H}_{M(H_2O)_6}$) of a water molecule in the hexa–aqua complex, as well as the ligand exchange rates from the first coordination sphere of the metal ion (k_{exch}).
[b] The numbers in brackets refer to CN = 8.
[c] High-spin electron configuration.

is known about the complexing properties of larger RNA and DNA structures (a summary of some physico-chemical properties of these four metal ions is given in Table 1). We have selected these four metal ions because (i) Mg^{2+} is *the* divalent metal ion freely available in every cell, (ii) Ca^{2+} is a neurotransmitter and is also present in millimolar concentrations within certain cell compartments (although highly regulated) [53–58], (iii) Mn^{2+} accelerates the catalytic rate of some ribozymes [45–47] and is often used as a probe in EPR [39,40] and NMR studies [59], and (iv) Cd^{2+} is also often considered a good mimic of Mg^{2+} and is thus commonly used in thio-rescue studies [60,61].

In the following sections, first a few examples describing the effects of the mentioned metal ions on the reactivity of a number of ribozymes are summarized in order to illustrate a selection of possibilities how metal ions might be used to regulate the reactivity of nucleic acids *in vivo*. In the next part, the binding properties of Mg^{2+}, Ca^{2+}, Mn^{2+}, and Cd^{2+} to the building blocks of nucleic acids are shortly reviewed and thereafter these data are compared to the results obtained from large RNA structures.

It is the aim of this review to draw parallels between the coordination chemistry of large nucleic acids and their building blocks, as well as to highlight the crucial differences in the coordinating properties of the four mentioned metal ions towards large DNAs as well as ribozymes and their building blocks. This will not only facilitate the interpretation of results from the field of RNA biochemistry, but it will also help to design experiments and sometimes even to predict the binding of metal ions to certain sites and their influence on the structure and activity of ribozymes.

2. Control of reaction rates by metal ions in DNAzymes and ribozymes

Several examples are known of naturally occurring ribozymes as well as of *in vitro* selected ribozymes and especially DNAzymes, which are either highly selective for a given kind of metal ion, where the assumption may be raised that Mg^{2+} is not the natural cofactor, or where the activity might be controlled by switching the kind of metal ion involved [8,45–52].

The hammerhead ribozyme was one of the first catalytic RNAs to be discovered and has been the focus of uncountable studies on its structure and the function of metal ions in catalysis. These data have been excellently reviewed [7,28,62–66] and therefore only the most important points regarding metal ion coordination will be mention here. The hammerhead ribozyme is active in the presence of millimolar amounts of Mg^{2+}, however, it retains its activity when Mg^{2+} is replaced by high molar amounts of monovalent cations like Li^+, Na^+ and also NH_4^+ [67–69]. As in addition, many experiments have indicated that binding of divalent metal ions only occurs 10–20 Å away from the cleavage site [69–72], these results have been repeatedly taken as evidence that metal ions are not directly involved in the catalytic step. However, these findings could also be interpreted as an indication that the role of these metal ions is more of an electrostatic nature, e.g. by stabilizing the transition state of the phosphodiester cleavage [7]. Even more interesting in the present context is the fact that the so-called minimal hammerhead ribozyme (which represents the best characterized hammerhead sequence) does not show its highest activity in the presence of Mg^{2+} but Mn^{2+} [73]. This observation is even more pronounced in the case of the recently described so-called extended hammerhead ribozyme [69,74–76], where so far the maximum cleavage rate has not been reached [45,46,74]. Interestingly, aside from Mn^{2+} also other transition metal ions like Co^{2+} or Ni^{2+}, as well as Zn^{2+} and Cd^{2+} lead to higher cleavage rates than Mg^{2+} [46]. It can therefore be speculated that the hammerhead ribozyme represents an example where Mg^{2+} is not the natural cofactor, but instead another divalent metal ion (perhaps even a redox active one) is used for *in vivo* function.

Another example of naturally occurring ribozymes where divalent metal ions have been shown to strongly influence the catalytic rate are self-splicing group II intron ribozymes [8,48,52]. Group II introns are very large catalytic RNAs and second in size only to the ribosome [8,77]. For every group II intron investigated today, Mg^{2+} has been shown to be the essential divalent metal ion that must not be omitted [8,23,25,77,78] as it is required for folding [79,80] and presumably also for catalysis [60,81–83]. In the case of the Sc.ai5γ group II intron from yeast, Mg^{2+} can be partially replaced by d^{10} metal ions like

Cd^{2+} or Zn^{2+} (and also Mn^{2+}) and retains activity, as is evident from so-called thio-rescue experiments [60,84,85]. However, when small amounts of Mg^{2+} are replaced by Ca^{2+}, an immediate drop in splicing activity can be observed [8,48,52]. This is highly interesting because Ca^{2+} plays an important role in living cells. Although tightly regulated due to its role as a neurotransmitter, Ca^{2+} concentrations can reach millimolar concentrations within certain cell compartments like mitochondria, which act as Ca^{2+} storage vesicles [53–58]. As Sc.ai5γ is located within the cytochrome oxidase 1 gene of mitochondrial DNA, it is reasonable to assume that the varying levels of freely available Ca^{2+} in this cell compartment also influence the splicing rate *in vivo* and therefore might be used to regulate other cellular reactions.

Examples exist where the metal ion specificity of naturally occurring ribozymes can be switched by appropriate mutations within the catalytic core. One such example encompasses group I introns. Usually, these large ribozymes have a strict requirement for either Mg^{2+} or Mn^{2+} to carry out catalytic activity [47]. This specificity could be switched completely to a selective requirement for Ca^{2+} by *in vitro* selection in both the *Tetrahymena* [86,87] as well as the *Azoarcus* group I intron [47]. However, it is unclear why a specificity exists in the first place and further how the few introduced single point mutations alter the metal ion specificity. Interestingly, two recent crystal structures of the *Azoarcus* group I intron [88,89] show that one of the two Mg^{2+} ions present in the catalytic core can be replaced by K^+. This indicates that indeed different metal ions compete for exactly the same site, although obviously their coordinating properties are different, but it is unknown how this affects catalysis.

In vitro selection experiments offer the opportunity to select nucleic acids with a high specificity for a certain kind of metal ion. One example is provided by variants of the so-called 8–17 DNAzymes [90–93], which are active in the presence of Mg^{2+}, Ca^{2+}, and Zn^{2+}. The cleavage rate under similar conditions thereby decreases in the order $Zn^{2+} \gg Ca^{2+} > Mg^{2+}$ [90,94,95]. Ironically, the variant 17E shows its highest activity in the presence of Pb^{2+}—a metal ion it was not selected for [49,96]. This DNAzyme has lately been further developed and is now used as a highly selective luminescent sensor for Pb^{2+} ions [96–100]. However, despite the intense research on this and related DNAzymes, to date no structural data are available that allow a conclusion regarding the coordination-chemical basis on which the different cleavage rates in the presence of different metal ions and the high selectivity for Pb^{2+} are founded. Obviously, a better knowledge of the coordination chemistry involved would allow to rationally design and/or improve further applications and selectivities.

To summarize, there is ample precedence in catalytic RNAs and DNAs that a high selectivity for metal ions is present and may by used to trigger and control the function of specific molecules. However, to the best of our knowledge no system has been described where the detailed effect of the metal ion switch is known on the atomic level. In the following section we will therefore summarize the available knowledge on the exact coordination modes of Mg^{2+}, Ca^{2+}, Mn^{2+}, and Cd^{2+} to the low-molecular weight building blocks of large nucleic acids.

3. Metal ion binding to the building blocks of RNA and DNA

3.1. Metal ion binding to mononucleotides

3.1.1. Comments on the structure and function of nucleotides in solution

Mononucleotides, either in their mono-, di- or triphosphorylated form, are very abundant in living cells serving a multitude of different functions (for their structures and labeling schemes see Fig. 1). In their triphosphorylated form (i.e. (d)NTPs with "N" being any nucleobase and "d" indicating the 2′-deoxy form of the ribose moiety) they constitute the building blocks for nucleic acid polymerases in the syntheses of RNA and DNA. In addition, ATP and to some extent also GTP serve as main energy sources for many enzymatic reactions in any organism and are further employed as neurotransmitters. These and other nucleotides are also important cofactors or substrates for enzymatic reactions including those where either the nucleobase (e.g. deaminases) [101,102] or the sugar moiety (e.g. ribonucleotide reductases) [103] are modified. No matter for which function,

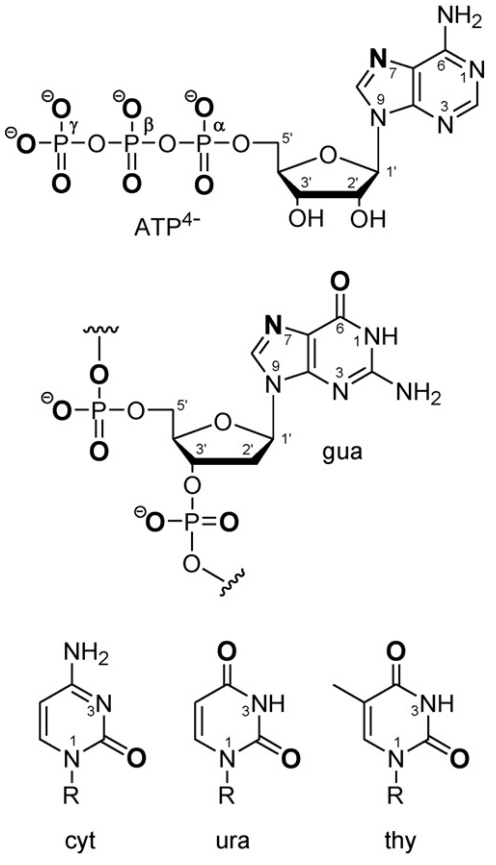

Fig. 1. Chemical structure of the five most common nucleobases in RNA and DNA. The structure of ATP^{4-} (with the adenine residue) is shown at the top together with its labeling scheme, 2′-deoxyguanosine (with the guanine moiety) is depicted in the middle together with the bridging phosphate groups as they occur in DNA, and the three pyrimidine nucleobases cytosine, uracil (in RNA) and thymine (instead of uracil in DNA) are drawn at the bottom. The major metal ion-coordinating atoms in nucleic acids are shown in bold.

nucleotides are always associated with metal ions due to the negatively charged phosphate residues.

However, metal ions are not only present for charge compensation, but they may also actively take part in enzymatic reactions and determine by their binding mode the path which a reaction follows [104–106]: simultaneous β-/γ-coordination of one of the two metal ions coordinated to the triphosphate chain of a (d)NTP (the second metal ion is coordinated to the α-phosphate) leads to cleavage of the anhydride bond between the α- and the β-phosphate groups (Fig. 1), a reaction also catalyzed by nucleic acid polymerases [107–109]. In contrast, α-/β-coordination of the first and γ-coordination of the second metal ion leads to the release of the terminal γ-phosphate group, as e.g. in kinases [105,110,111].

With an excess of metal ions and in the absence of further coordinating ligands, such as a protein scaffold, the latter α-/β- and γ-coordination mode prevails in equilibrium in solution [104,105,112]. Hence, mainly hydrolysis to the nucleoside diphosphate and free monophosphate (i.e. kinase activity) will occur [104]. It is remarkable that even in such simple systems, the rate of hydrolysis is increased tremendously if a mixture of two different metal ions (e.g. Mg^{2+} and Cu^{2+}) is used [112]. This illustrates nicely that the two coordinated metal ions serve different purposes, thus giving rise to synergism, and that even in such simple systems discrimination among metal ions occurs. One may therefore speculate if not also within more complex systems like ribozymes different kinds of metal ions can coordinate to specific binding pockets leading to synergistic effects.

3.1.2. Stability of metal ion–nucleotide complexes in solution

Complex formation of any metal ion with a nucleotide can be described by the following equilibrium:

$$M^{2+} + NXP^{y-} \rightleftarrows M(NXP)^{(y-2)-} \tag{1a}$$

$$K^{M}_{M(NXP)} = \frac{[M(NXP)^{(y-2)-}]}{[M^{2+}][NXP^{y-}]} \tag{1b}$$

NXP^{y-} denotes the mono-, di-, or triphosphate form of any nucleotide or 2′-deoxy nucleotide, whereby "y" is the corresponding charge value ($y=2$ for the nucleoside mono-, $y=3$ for the di-, and $y=4$ for the triphosphate). The competition of a metal ion with the proton bound at the terminal phosphate group needs not to be considered in this equilibrium. Such a proton is released with a pK_a value of about 6.2 for nucleoside 5′-monophosphates, $H(NMP)^-$, and 6.50 ± 0.05 for nucleoside 5′-triphosphates, $H(NTP)^{3-}$ [113–116], and has thus hardly any influence on the extent of metal ion coordination in the physiological pH range of about 7.5 (for more details see e.g. Refs. [115,117,118]). Irrespective of the number of phosphate groups present at the 5′-end, this residue is always the primary binding site for alkaline, alkaline earth, and 3d-transition metal ions, as well as Zn^{2+} or Cd^{2+}.

In the case of purine-nucleoside 5′-phosphates a further, namely an intramolecular equilibrium exists: the phosphate-coordinated metal ion can form a macrochelate by interacting with N7 of the nucleobase moiety. Depending on the kind of nucleotide and metal ion these interactions may occur in an inner- or outersphere manner [113] (see also Section 4). If not explicitely mentioned, in the context of this review we do commonly not distinguish between these two binding modes as 'global' stability constants are measured by potentiometric pH titrations [113]. Such macrochelate formation gives rise to the following intramolecular equilibrium (2):

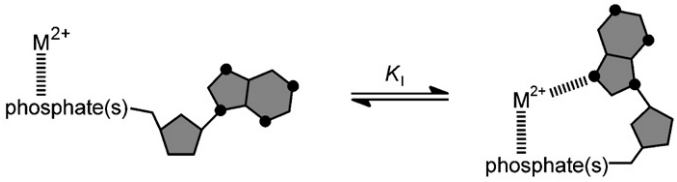

(2)

The formation degree of the macrochelated or "closed" species, $M(NXP)_{cl}^{(y-2)-}$ on the right side of equilibrium (2), is thereby independent of the total complex concentration because it is an intramolecular equilibrium. Therefore, its equilibrium constant K_I, as defined by Eq. (3), is dimensionless [117,119,120]:

$$K_I = \frac{[M(NXP)_{cl}^{(y-2)-}]}{[M(NXP)_{op}^{(y-2)-}]} \tag{3}$$

$M(NXP)_{op}^{(y-2)-}$ refers to the "open", i.e. solely phosphate-coordinated, species, and hence equilibrium (1a) may be rewritten as given in (4):

$$M^{2+} + NXP^{y-} \overset{K^{M}_{M(NXP)_{op}}}{\rightleftharpoons} M(NXP)_{op}^{(y-2)-} \overset{K_I}{\rightleftharpoons} M(NXP)_{cl}^{(y-2)-} \tag{4}$$

$K^{M}_{M(NXP)_{op}}$ thereby represents the stability constant of the open species. The stability increase, $\log \Delta$, due to macrochelate formation is defined by Eq. (5):

$$\log \Delta = \log \Delta_{M(NXP)} = \log K^{M}_{M(NXP)} - \log K^{M}_{M(NXP)_{op}} \tag{5}$$

and the intramolecular equilibrium constant K_I can then be calculated with Eq. (6):

$$K_I = \frac{K^{M}_{M(NXP)}}{K^{M}_{M(NXP)_{op}}} - 1 = 10^{\log \Delta} - 1 \tag{6}$$

Based on the value of K_I, the formation degree of the closed species can be calculated for any kind of nucleotide-metal ion complex by Eq. (7):

$$\%M(NXP)_{cl}^{(y-2)-} = \frac{K_I}{1 + K_I} \times 100 \tag{7}$$

These $\%M(NXP)_{cl}^{(y-2)-}$ values for the various metal ions discussed here, i.e. Mg^{2+}, Ca^{2+}, Mn^{2+}, and Cd^{2+}, are summarized in Tables 2 and 3 for several purine-nucleotide systems. Each value represents the tendency of the specific metal ion for macrochelate formation, or in other words, its affinity for the N7 position when already bound to the phosphate terminus (for a more detailed derivation of Eqs. (3)–(7), please refer to Refs. [119–121]).

Table 2
Experimentally determined stability constants, $K^{M}_{M(NXP)}$, for $M(NXP)^{(y-2)-}$ complexes, i.e. including the contribution of macrochelate formation, and calculated stability constants, $K^{M}_{M(NXP)_{op}}$, for the corresponding isomers with a sole phosphate coordination of Mg^{2+} and Ca^{2+} [a]

NXP^{y-}	Mg^{2+}				Ca^{2+}				
	$\log K^{M}_{M(NXP)}$	$\log K^{M}_{M(NXP)_{op}}$	K_I	$\%M(NXP)_{cl}{}^{(y-2)-}$	$\log K^{M}_{M(NXP)}$	$\log K^{M}_{M(NXP)_{op}}$	K_I	$\%M(NXP)_{cl}{}^{(y-2)-}$	References
AMP^{2-}	1.62 ± 0.04	1.56 ± 0.03	0.15 ± 0.13	13 ± 10	1.48 ± 0.03	1.45 ± 0.05	0.07 ± 0.14	0 (7 ± 13)	[118,122]
ADP^{3-}	3.36 ± 0.03	3.30 ± 0.03	0.15 ± 0.11	13 ± 9	2.95 ± 0.02	2.91 ± 0.03	0.10 ± 0.09	9 ± 8	[118]
ATP^{4-}	4.29 ± 0.03	4.21 ± 0.04	0.20 ± 0.14	17 ± 10	3.91 ± 0.03	3.84 ± 0.05	0.17 ± 0.16	15 ± 12	[116,165]
GMP^{2-}	1.73 ± 0.03	1.57 ± 0.03	0.45 ± 0.14	31 ± 7	1.57 ± 0.03	1.45 ± 0.05	0.32 ± 0.18	24 ± 10	[122]
GDP^{3-}	3.39 ± 0.04	3.29 ± 0.03	0.26 ± 0.14	21 ± 9	3.05 ± 0.05	2.90 ± 0.03	0.41 ± 0.19	29 ± 19	[117,176]
GTP^{4-}	4.31 ± 0.04	4.21 ± 0.04	0.26 ± 0.17	21 ± 11	3.96 ± 0.03	3.84 ± 0.05	0.32 ± 0.18	24 ± 10	[165]

[a] The extent of intramolecular macrochelate formation in the various $M(NXP)^{(y-2)-}$ complexes is given in columns 4 and 5 as well as 8 and 9 (see also text in Section 3.1). All data refer to aqueous solution at 25 °C and $I = 0.1$ M ($NaNO_3$). All error limits given are three times the standard error of the mean value or the sum of the probable systematic errors, whichever is larger.

Table 3
Experimentally determined stability constants, $K^{M}_{M(NXP)}$, for $M(NXP)^{(y-2)-}$ complexes, i.e. including the contribution of macrochelate formation, and calculated stability constants, $K^{M}_{M(NXP)_{op}}$, for the corresponding isomers with a sole phosphate coordination of Mn^{2+} and Cd^{2+}. The extent of intramolecular macrochelate formation in the various $M(NXP)^{(y-2)-}$ complexes is given in columns 4 and 5 as well as 8 and 9 (see also text in Section 3.1)[a]

NXP^{y-}	Mn^{2+}				Cd^{2+}				
	$\log K^{M}_{M(NXP)}$	$\log K^{M}_{M(NXP)_{op}}$	K_I	$\%M(NXP)_{cl}{}^{(y-2)-}$	$\log K^{M}_{M(NXP)}$	$\log K^{M}_{M(NXP)_{op}}$	K_I	$\%M(NXP)_{cl}{}^{(y-2)-}$	References
AMP^{2-}	2.23 ± 0.02	2.16 ± 0.05	0.17 ± 0.15	15 ± 11	2.74 ± 0.05	2.44 ± 0.05	1.00 ± 0.32	50 ± 8	[118,122]
ADP^{3-}	4.22 ± 0.02	4.12 ± 0.03	0.26 ± 0.10	21 ± 7	4.63 ± 0.04	4.27 ± 0.03	1.29 ± 0.26	56 ± 5	[118]
ATP^{4-}	5.01 ± 0.08	4.93 ± 0.03	0.20 ± 0.22	17 ± 15	5.34 ± 0.03	5.07 ± 0.03	0.86 ± 0.17	46 ± 5	[116,165]
GMP^{2-}	2.42 ± 0.05	2.17 ± 0.05	0.78 ± 0.29	44 ± 9	3.25 ± 0.03	2.46 ± 0.05	5.17 ± 0.83	84 ± 2	[122]
GDP^{3-}	4.35 ± 0.06	4.11 ± 0.03	0.74 ± 0.27	42 ± 9	4.86 ± 0.03	4.25 ± 0.03	3.07 ± 0.40	75 ± 2	[117,176]
GTP^{4-}	5.36 ± 0.03	4.93 ± 0.03	1.69 ± 0.25	63 ± 3	5.82 ± 0.05	5.07 ± 0.03	4.62 ± 0.78	82 ± 2	[165]

[a] All data refer to aqueous solution at 25 °C and $I = 0.1$ M ($NaNO_3$). All error limits given are three times the standard error of the mean value or the sum of the probable systematic errors, whichever is larger.

Comparison of the data accumulated in Tables 2 and 3 reveals the following distinct differences between Mg^{2+}, Ca^{2+}, Mn^{2+}, and Cd^{2+} in terms of their overall binding affinity in general, as well as their ability to simultaneously coordinate to the phosphate group(s) and the purine N7 position, i.e. to form a macrochelate:

(i) For each of the four metal ions discussed here, the stability constants $\log K^{M}_{M(NXP)_{op}}$, representing the pure phosphate coordination of a given metal ion in a $M(NXP)^{(y-2)-}$ complex, increase in the order of $NMP^{2-} < NDP^{3-} < NTP^{4-}$ (Fig. 2). This is certainly to be expected as an additional stabilization by chelate formation becomes possible with an increasing number of phosphate units. Furthermore, the negative charge increases by one unit with each additional phosphate group. Thereby, the nature of the nucleobase has virtually no influence on the binding affinity of a certain metal ion to the 5′-phosphate chain alone, e.g. the $\log K^{M}_{M(NXP)_{op}}$ values for Mg^{2+} binding to AMP^{2-} and GMP^{2-} are the same within their error limits. The very minor difference of 0.01 log unit is due to a similarly small difference in phosphate basicity (e.g. $pK^{H}_{H(AMP)} = 6.21 \pm 0.01$ and $pK^{H}_{H(GMP)} = 6.25 \pm 0.02$ [122]. Consequently, also in a large nucleic acid structure, each monophos-

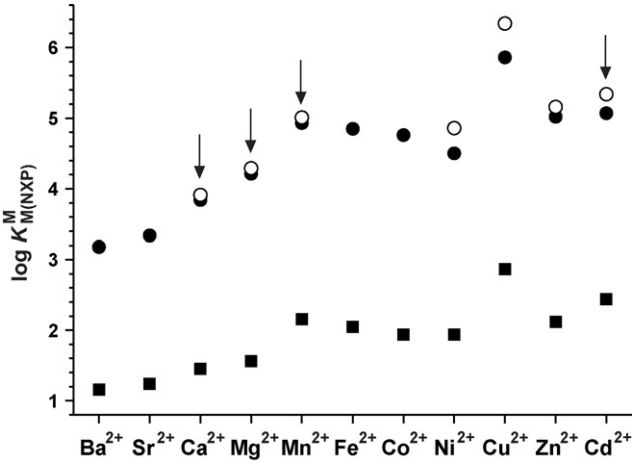

Fig. 2. Plots of the logarithms of the stability constants for the complexes of alkaline earth and divalent 3d-transition metal ions as well as Zn^{2+} and Cd^{2+} formed with the monophosphate ($\log K^{M}_{M(AMP)_{op}}$, ■) or triphosphate residue ($\log K^{M}_{M(ATP)_{op}}$, ●) and with ATP^{4-} ($\log K^{M}_{M(ATP)}$, ○) [116,118,122,165]. The stabilities of the complexes including the four metal ions mainly discussed here, i.e. Mg^{2+}, Ca^{2+}, Mn^{2+}, and Cd^{2+}, are indicated by arrows. The stabilities are plotted from left-to-right according to the Irving–Williams series [123,124,166] (which is not strictly followed for phosph(on)ate ligands) [158] and the *Stability Ruler* proposed by Martin [125–127].

phate diester group is expected to exhibit the same affinity towards a given metal ion irrespective of its position within the primary sequence and the attached nucleobase. It follows that other factors, i.e. additional binding sites or steric restrictions, must be responsible for any discrimination observed.

(ii) For all NXP^{y-} ligands, the stability constant $\log K^{M}_{M(NXP)_{op}}$ of the $M(NXP)_{op}{}^{(y-2)-}$ complexes increases in the order of $Ca^{2+} < Mg^{2+} < Mn^{2+} < Cd^{2+}$. The lower stability of the Ca^{2+} complexes compared to those of Mg^{2+} can thereby be explained by the larger ionic radius of Ca^{2+} (72 pm versus 100 pm for coordination number CN = 6). The affinities of Mn^{2+} and Cd^{2+} are clearly higher compared to Mg^{2+} by (on average) about 0.7 and 0.9 log units, respectively, which agrees with the position of Mn^{2+} within the Irving–Williams series [117,123,124] (see Fig. 2). The slightly higher stability of the Cd^{2+} complexes compared to the corresponding Mn^{2+} complexes is well in accord with the *Stability Ruler* of Martin [125–127]. The accumulated data in Tables 2 and 3 show that the different nature of a metal ion can have an effect in the same order as that of a further phosphate group, e.g. $\log K^{Mg}_{Mg(ATP)_{op}} \approx \log K^{Cd}_{Cd(ADP)_{op}}$.

(iii) Macrochelate formation, i.e. the additional coordination of the phosphate-bound metal ion to the N7 position of the purine-moiety (Eq. (2)), is more distinct with guanine than with adenine (Tables 2 and 3) and most likely due to the fact that the carbonyl O6 may participate via an outersphere interaction in metal ion binding (Fig. 3) [122,128,129]. On the contrary, the exocyclic $N6H_2$ group of the adenine nucleobase is known to have an inhibiting effect on metal ion coordination at its N7 position [130]. In contrast to earlier conclusions [128] the basicity of N7 in guanine and adenine residues is comparable and therefore has no influence on the metal ion binding affinity, i.e. for 9-methylguanine $pK^{H}_{H(9MeG)} = 3.11 \pm 0.06$ and for 9-methyladenine $pK^{H}_{H-N7-9\text{-}MeA-N1} = 2.96 \pm 0.10$ (micro acidity constant) [131].

(iv) In the case of the adenine complexes $M(AXP)^{(y-2)-}$, the extent of macrochelate formation is within the error limits independent of the number of phosphate groups present at the 5′-end of the nucleoside. This parity in the extent of macrochelate formation occurs despite the fact that the absolute stabilities of the complexes differ drastically. The same observation is made with the Mg^{2+} and Ca^{2+} complexes of the guanosine derivatives. However, for the Mn^{2+} complexes the order $GMP^{2-} \approx GDP^{3-} < GTP^{4-}$ and for the Cd^{2+} complexes the order $GDP^{3-} < GMP^{2-} \approx GTP^{4-}$ is found. In the latter cases, the differences are small but most likely they are real and they might be a reflection of the various degrees of outersphere complexation [104,113,128].

(v) The four metal ions discussed have clearly different abilities to form macrochelates: a comparison shows that Ca^{2+} forms only very small amounts of macrochelates (if at all). Mg^{2+} and Mn^{2+} are comparable in their affinity towards N7 of adenine and both have a moderate binding tendency with formation degrees of up to 20% for the $M(NXP)_{cl}{}^{(y-2)-}$ species. With guanine, Mn^{2+} shows a higher affinity towards N7 than Mg^{2+}, which is probably due to more innersphere binding of Mn^{2+}. Cd^{2+} clearly is the best suited metal ion for macrochelate formation with all purine nucleotides with formation degrees of about 50% or more.

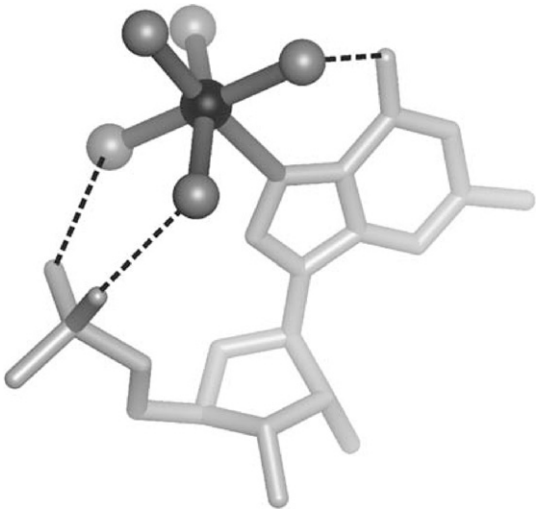

Fig. 3. Inner- and outersphere coordination of Cd^{2+} in the Cd(GMP)$(H_2O)_5 \cdot 3H_2O$ complex. The Cd^{2+} ion is directly coordinated to N7 of the guanine residue and additionally forms three hydrogen bonds via three coordinated water molecules to the phosphate group and the carbonyl oxygen O6. The Cd^{2+} ion is shown as a black sphere, the coordinated water molecules as grey spheres, and the nucleotide in lighter grey. The three hydrogen bonds are indicated by dashed lines. Three further water molecules present in the crystal structure are omitted for clarity. This figure has been prepared with MOLMOL [167] based on the coordinate file AGOPCD [129].

Having discussed the structures of metal ion complexes of mononucleotides in solution and the differences posed by the four mentioned metal ions, it will now be interesting to see if these features are also reflected in the solid–state structures of such complexes.

3.1.3. Insights from crystallography

There are quite a number of crystal structures of mononucleotides, which have been excellently reviewed by Aoki [132,133]. Most of these structures contain Na^+ as a metal ion, and thus shall not be discussed here as we are concentrating again on the four metal ions Mg^{2+}, Ca^{2+}, Mn^{2+}, and Cd^{2+}.

Several structures of nucleoside 5′-monophosphates are available with Cd^{2+} and Ca^{2+}, e.g. of Cd^{2+} with CMP^{2-} and $dCMP^{2-}$ [134–136], which are of a polymeric nature: in all cases Cd^{2+} shows at least two innersphere contacts (plus one or more outersphere interactions) to a phosphate group (Fig. 4A). A further prominent site of innersphere coordination is the N3 nitrogen of the pyrimidine moiety (Fig. 4A), which is usually not available for metal ion binding in double-stranded nucleic acids as it is involved in hydrogen bonding. Interestingly, only

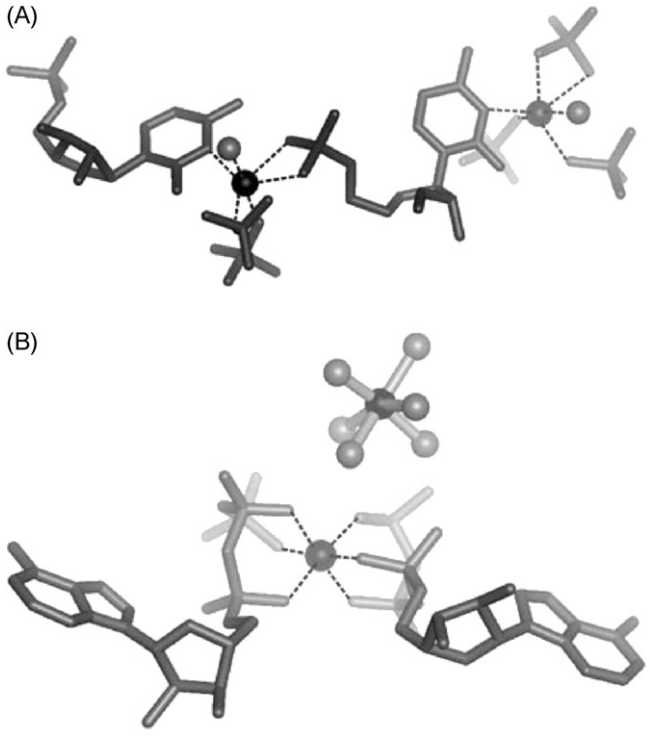

Fig. 4. X-ray structures of M^{2+} complexes with mononucleotides. (A) Crystal structure of CMP^{2-} with Cd^{2+}. The metal ion is coordinated to N3 of a cytosine residue, one water molecule, and four phosphate-oxygen atoms of three other CMP^{2-} molecules leading to a polymeric structure. (B) In the $[Mg(HATP)_2]^{4-}$ complex, a fully dehydrated Mg^{2+} ion bridges the triphosphate chains of two ATP molecules thereby coordinating to every phosphate group. A second Mg^{2+} is present in its hexahydrate form. The octahedral coordination spheres of Cd^{2+} and Mg^{2+} bound to the nucleotides are indicated by dashed lines. Additional water molecules and the bis(2-pyridyl)-amine ligand present (in B) are omitted for clarity. This figure has been prepared with MOLMOL [167] based on the coordinate files ACMPCD (Cd^{2+}/CMP^{2-}) [134] and DECDIY (Mg^{2+}/ATP^{4-}) [146].

innersphere but no outersphere interaction to N3 can be observed in any of the Cd^{2+} structures. In contrast, the carbonyl oxygen O2 shows no discrimination between a direct coordination or binding via a water molecule to the Cd^{2+} ion.

Similar observations have been made with UMP^{2-}, $dUMP^{2-}$, or $dTMP^{2-}$ and Cd^{2+} [137,138] or Ca^{2+} [139,140]: Again, at least two innersphere and two outersphere contacts of the Cd^{2+} (or Ca^{2+}) to phosphate oxygens are present. Surprisingly at first sight, no interactions are observed with the two carbonyl oxygens, O2 and O4. As the N3 position in uracil or thymine is blocked by a proton, this finding is a strong indication that the $Cd^{2+}(OH_2)\cdots O{=}C$ interactions (either inner- or outersphere) are so weak that they can only be observed, when the much stronger $Cd^{2+}\cdots N3$ bond is formed as is the case with cytosine where also additional chelate formation results [141,142].

GMP^{2-} has been crystallized in the presence of Mn^{2+} [143,144] or Cd^{2+} [129]. In both cases, the metal ion is bound to the N7 position by innersphere coordination (unfortunately, in the case of the MnGMP structure no coordinates are available for a more detailed analysis). The five water ligands of the octahedral Cd^{2+} ion, which is coordinated to N7 (Fig. 3), show an extensive hydrogen bonding network to seven (!) phosphate oxygens, as well as to the O6, N1H and $N2H_2$ sites of the guanine nucleobase [129].

The Cd^{2+} structures discussed above confirm the findings from the solution studies described in Section 3.1.2 that this metal ion shows indeed a high affinity towards nitrogen sites. Nevertheless, the innersphere coordination to phosphate groups in the case of the pyrimidine 5′-monophosphate systems as well as the extensive network of outersphere interactions to several phosphate residues in the GMP system demonstrate the high affinity between phosphate moieties and Cd^{2+}.

ATP has been crystallized several times with Mg^{2+} [145–147] and Ca^{2+} [145–147] and once each with Mn^{2+} [148] and Cd^{2+} [147] and should thus provide an ideal basis for a comparison of the coordination tendencies of these four metal ions. However, all structures are virtually identical as a superposition of the nucleotide and the metal ions demonstrates (not shown). A fully dehydrated metal ion bridges the triphosphate chains of two ATP molecules thereby coordinating to every phosphate group (Fig. 4B). The second metal ion present in the crystal structures is in its hexahydrate form showing an extensive hydrogen bonding network to further phosphate groups, a sugar residue, as well as a water molecule. Obviously this finding is not in perfect agreement with the results of the solution studies. While both methods demonstrate that the triphosphate group is the primary binding site, the solution studies show in addition a discrimination between the various metal ions in their tendency towards macrochelate formation with N7. A reason for this discrepancy is certainly the effect of crystal packing, as hydrogen bonding between pairs of adenine nucleobases as well as between the adenine moieties and neighboring triphosphate groups is observed. In addition, stacking interactions between the adenine nucleobase and heteroaromatic amines, like 2,2′-dipyridylamine used for crystallization, are observed. All these interactions are likely to shield the purine nucleobase from additional metal ion interactions, as observed in solution.

To summarize, some crystal structures of metal ion complexes with mononucleotides confirm nicely the results from solution studies, others do so to a lesser extent. In general, there are only very few structures available of complexes formed with different metal ions and the most common nucleotides. Consequently, this makes it difficult (or actually impossible) to draw definite conclusions from such comparisons. It is evident that it would be very advantageous to obtain more such structures of complexes, crystallized under different conditions.

3.2. Metal ion binding to dinucleotides

The mononucleotides discussed in Section 3.1 distinguish themselves from the situation in nucleic acids in that they lack the single negatively charged bridging phosphate diester group. One of the simplest systems containing such a phosphate diester is a dinucleotide. The direct determination of stability constants of metal ion complexes formed with such a bridging phosphate is very difficult because no competition for binding occurs between protons and metal ions within the experimentally accessible pH range for potentiometric pH titrations. This means that in the

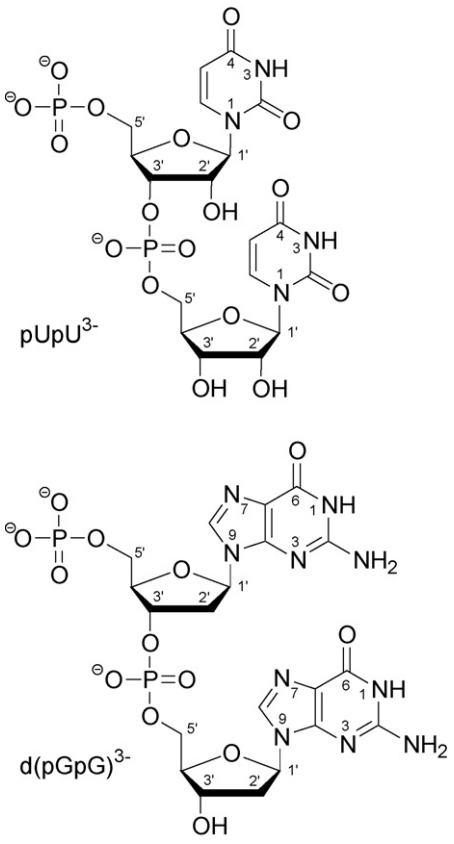

Fig. 5. Chemical structure of the two dinucleotides discussed in this review, i.e. $pUpU^{3-}$ (top) and $d(pGpG)^{3-}$ (bottom), together with their numbering schemes.

physiological pH range the phosphate unit is always deprotonated and in principle freely accessible for metal ions [149,150]. To the best of our knowledge only two studies exist that quantify the coordination of M^{2+} ions to a bridging phosphate [150,151]. These two studies with $pUpU^{3-}$ and $d(pGpG)^{3-}$ (Fig. 5) that both contain an additional 5′-terminal phosphate group, therefore also quantify the simultaneous coordination of one metal ion to two neighboring phosphate units, which is a key feature of ribozyme structure and function.

Naturally, binding equilibria of metal ions with dinucleotides are more complicated than with mononucleotides. The 5′-terminal phosphate group remains the primary binding site due to its twofold negative charge. In case of the dinucleotide $d(pGpG)^{3-}$ this leads to the species $M[d(pGpG)]_{op}^{-}$. For a metal ion bound to the terminal phosphate group of a purine dinucleotide, two possibilities for further coordination within the molecule are feasible. As depicted in the following equilibrium,

the metal ion can additionally coordinate either to the bridging phosphate group, resulting in $M[d(pGpG)]_{cl/PO}^{-}$, or to the N7 position of the same nucleotide, yielding $M[d(pGpG)]_{cl/N7}^{-}$ [151]. For coordination to $pUpU^{3-}$ only macrochelate formation with the bridging phosphate group is possible, i.e. the left side of equilibrium (8), as pyrimidine nucleobases in their dominating *anti* conformation offer no additional binding site for a 5′-phosphate bound metal ion [117,150].

In analogy to the situation in equilibrium (2), also here the two corresponding equilibrium constants $K_{I/PO}$ and $K_{I/N7}$ are dimensionless and macrochelate formation is again independent of complex concentration. It is obvious that in cases like $d(pGpG)^{3-}$, a competition is taking place between the bridging phosphate and the N7 nitrogen of the 5′-nucleotide for binding of the second site. The extent to which one of the two internal equilibriums is favored over the other is therefore only dependent on the nature of the metal ion, i.e. its preference for an oxygen or nitrogen donor site, respectively.

Metal ion coordination to $pUpU^{3-}$ can be used to quantify the ability of different metal ions to bridge the two phosphate groups in any dinucleotide and has been investigated with Mg^{2+}, Mn^{2+}, Cd^{2+}, Zn^{2+}, and Pb^{2+}: out of these five metal ions, Mg^{2+}, Mn^{2+}, and Cd^{2+} all show the same slight stability increase of $\log \Delta = 0.24 \pm 0.04$ (3σ), which is solely due to the additional negative charge within the molecule compared to UMP^{2-} [150]. Therefore, none of these three metal ions forms macrochelated species or only traces thereof. This is different with Zn^{2+} and Pb^{2+}. About 25% of the Zn^{2+} complex is present as the closed species $Zn[pUpU]_{cl/PO}^{-}$ ($\log \Delta = 0.37 \pm 0.07$ (3σ)) and in case of Pb^{2+} about 93% is in the macrochelated form ($\log \Delta = 1.40 \pm 0.26$ (3σ)) [150]. These results are actually well in line with the *Stability Ruler* proposed by Martin [125–127] for the interaction of metal ions with simple oxygen donors such as oxalate and thus they illustrate further already at this point that a "scale-up" of such observations from small to larger molecules is possible and also valid.

For the complexes $M[d(pGpG)]^{-}$ ($M^{2+} = Mg^{2+}$, Zn^{2+}, Cd^{2+}, and Pb^{2+}) macrochelate formation can be observed in all systems [151]. Mg^{2+} and Cd^{2+} both form exclusively the N7 coordinated macrochelate $M[d(pGpG)]_{cl/N7}^{-}$ with surprisingly high formation degrees of about 72 and 94%, respectively [151]. These formation degrees are somewhat larger than those observed for the corresponding M(GMP) and M(dGMP) species [122,152]. A possible reason for this result is most likely a partial preorientation of the dinucleotide due to an intramolecu-

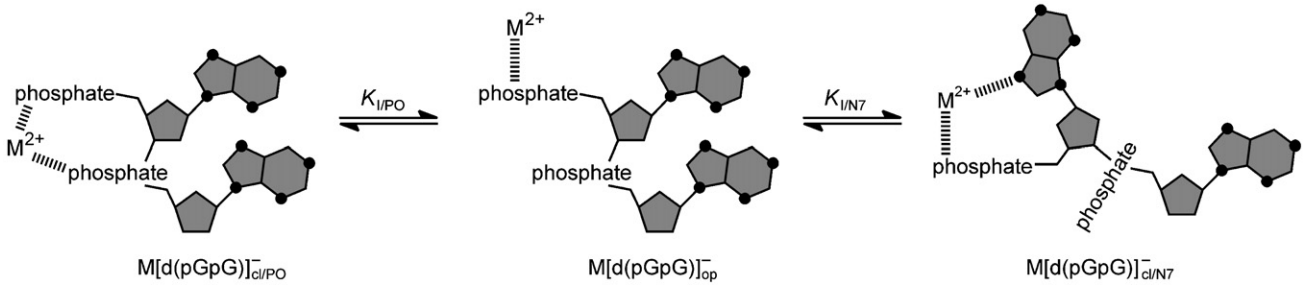

(8)

lar guanine-guanine stack occurring in $d(pGpG)^{3-}$ (see Section 3.3). In accord herewith is the slightly smaller formation degree of the $Pb[d(pGpG)]_{cl/PO}^{-}$ species compared to $Pb[pGpG]_{cl/PO}^{-}$ (see below) as the guanine-guanine base-stacking is expected to inhibit the flexibility of the dinucleotide needed for the formation of the 10-membered phosphate–phosphate chelate. It is very well feasible that such a preorientation via nucleobase stacking (and other interactions like hydrogen bonding) is very important for the formation of a metal ion binding pocket in larger nucleic acids (for a more detailed discussion see Section 3.3).

For the above-mentioned $M[d(pGpG)]_{cl/N7}^{-}$ complexes, a distinction between innersphere and outersphere binding is not possible, the latter being expected to occur especially with Mg^{2+}. Zn^{2+} forms to a large extent the N7-bound species $Zn[d(pGpG)]_{cl/N7}^{-}$ as well, but additionally, also a lower percentage of the bridged bis-phosphate chelate $Zn[d(pGpG)]_{cl/N7}^{-}$ is present [151]. In combination with the data from $pUpU^{3-}$ the conclusion seems justified that as soon as a N7 site is available for coordination, Zn^{2+} prefers this ring nitrogen over a second phosphate binding. Again, Pb^{2+} shows a very high affinity towards oxygen donor ligands and consequently, the phosphate bridged complex $Pd[d(pGpG)]_{cl/PO}^{-}$ is exclusively observed with a formation degree of $84 \pm 6\%$ [151]. Most likely this overwhelming preference for phosphate binding over N7 coordination is also true for Ca^{2+} [151,153]. This would mean that Mg^{2+} and Ca^{2+} show a rather different binding behavior towards neighboring phosphate groups leading to different coordination environments and consequently also to different possible changes in local structure which might also affect catalysis—something which is indeed observed in group II intron ribozymes (see Section 2) [8,52].

As shown above for mononucleotides, the phosphate residue behaves identically in its binding property to a given metal ion irrespective of the nucleobase attached to the (deoxy)ribose moiety (Tables 2 and 3), i.e. every metal ion exhibits its specific binding affinity dependent on its preference for oxygen ligands and its position in the Periodic Table. In contrast, the two dinucleotides $pUpU^{3-}$ and $d(pGpG)^{3-}$, and most likely also others, behave differently: The coordinating properties of metal ions towards two neighboring phosphate groups depend on their affinity for oxygen ligands (compare the left part of equilibrium (8)) and consequently different local structures can be formed even without the direct participation of nucleobases as binding sites.

3.3. The effect of structural preorientation in dinucleotides on metal ion binding

Aside from interactions with metal ions, the structures of large and complex RNAs (and DNAs) are predominantly determined by internucleotide interactions like hydrogen bonding and stacking between the aromatic nucleobase moieties. As stacking interactions between purines are much stronger than between pyrimidines [154–157], one may expect that in the dinucleotide $d(pGpG)^{3-}$ some orientation between the two guanine planes occurs, whereas in $pUpU^{3-}$ such stacking interactions are expected to be absent (or much smaller) [154,155]. Such an orientation between the two nucleotide units should also affect the relative positioning of the two phosphate groups to each other as well as the positions of the N7 sites in relation to the phosphate moieties. It will now be interesting to see, if in some way such an orientation is reflected in the strengths of metal ion binding, i.e. macrochelate formation as expressed in equilibrium (8). Naturally, such insights into the question of a possible preorientation are of relevance for nucleic acid structures and the coordination of a metal ion at a specific site.

For the evaluation of such effects regarding the orientation of subunits in space, one needs to compare the charge-corrected stability enhancements due to macrochelate formation (equilibrium (8)) for the $M[d(pGpG)]^{-}$ complexes [151] with those of the corresponding M(dGMP) species [152] (available for $M^{2+} = Mg^{2+}$, Zn^{2+} or Cd^{2+}; the required data are summarized in Table 4) [122,151,152,158]. Indeed, there is clearly an extra stability enhancement for the $M[d(pGpG)]^{-}$ complexes, which amounts on average to $\Delta \log \Delta^{*}_{M/d(pGpG)/dGMP/av} = \log \Delta^{*}_{M/d(pGpG)/cor} - \log \Delta_{M/dGMP} = 0.31 \pm 0.07$ (Table 4, column 5). One may now attribute this "extra" stability enhancement to a preorientation of the $d(pGpG)^{3-}$ ligand, i.e. an intramolecular head-to-head stacking between the two purine moieties. This stacking arrangement would then facilitate macrochelate formation of the metal ion coordinated at the terminal phosphate group with the N7 site of the same dG. Even an additional coordination to the 3′-neighboring dG might be feasible, probably (partly) in an outersphere manner. Indeed, such a "three-point interaction" with two consecutive purines is sterically possible as the results for Mg^{2+} coordination in the ribosome demonstrate (see Fig. 6 and Section 4.1).

If the above assumption of a preorientation for the $d(pGpG)^{3-}$ ligand in solution is correct, then the formation

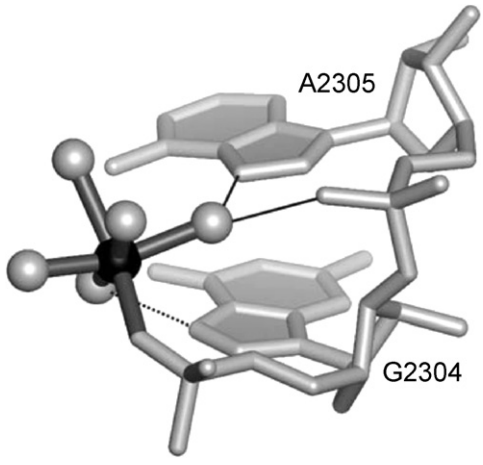

Fig. 6. Three and four point interaction of Mg^{2+} with two consecutive purines in the ribosome. The Mg^{2+} is shown as a black sphere and is innersphere coordinated to the R_P phosphate oxygen of G2304 and five water molecules. Hydrogen bonding, i.e. outersphere coordination (see also Fig. 7), of one water molecule is observed to the R_P phosphate oxygen and the N7 of the 3′-nucleotide A2305, thus forming a three-point interaction (solid thin lines). A second water molecules forms a further hydrogen bond to N7 of G2304 (thin dotted line), thus completing the fourpoint interaction (see also Sections 3.2, 3.3 and 4.1, as well as Figs. 8 and 9). This figure shows the coordination environment of Mg^{2+} no. 21 in the large ribosomal subunit of *H. marismortui* [19] (see also Fig. 8B) and has been prepared with MOLMOL [167] based on the PDB file 1S72 [19].

Table 4
Comparison of the stability enhancements observed for several M^{2+} complexes of $d(pGpG)^{3-}$, $dGMP^{2-}$, and GMP^{2-} due to the interactions of the phosphate-coordinated metal ions with the guanine residues. All data refer to aqueous solution at 25 °C and $I = 0.1$ M ($NaNO_3$)[a]

	$\log \Delta^*_{M/d(pGpG)/cor}$	$\log \Delta_{M/dGMP}$	$\log \Delta_{M/GMP}$	$\Delta \log \Delta^*_{M/d(pGpG)/dGMP}$
Mg^{2+}	0.55 ± 0.08	0.23 ± 0.05	0.16 ± 0.04	0.32 ± 0.09[b]
Zn^{2+}	1.16 ± 0.09[c]	0.84 ± 0.08	0.69 ± 0.07	0.32 ± 0.12[b]
Cd^{2+}	1.21 ± 0.09	0.92 ± 0.11[d]	0.79 ± 0.06	0.29 ± 0.14[b]
Cu^{2+}		1.14 ± 0.07	0.97 ± 0.07	

[a] For the error limits see footnote 'a' in Tables 2 and 3. The results listed in column 2 (charge-corrected stability enhancements due to $M[d(pGpG)]_{cl/N7}^-$ formation), column 3 (due to $M(dGMP)_{cl}$), and column 4 (due to $M(GMP)_{cl}$) are from Refs. [122,151,152], respectively.

[b] The three values in column five give on average $\Delta \log \Delta^*_{M/d(pGpG)/dGMP/av} = 0.31 \pm 0.07$. If one totally attributes this extra stability enhancement observed for the $M[d(pGpG)]^-$ complexes, compared to the situation in M(dGMP), to a preformed favorable orientation of the $d(pGpG)^{3-}$ ligand, one may estimate [158] the extent of intramolecular stacking between the purine residues in $d(pGpG)^{3-}$ and obtains for the intramolecular constant $K_{I/stack} = 10^{\Delta \log \Delta^*} - 1 = 1.04$ and for the percentage of the stacked species, % $[d(pGpG)]_{stack}^{3-} = 51\%$. See also the discussion in the text of Section 3.3.

[c] This value is corrected for the extent of the interaction with the neighboring phosphate group, i.e. from $K_{I/N7} = 13.44 \pm 3.08$ follows the above value [151].

[d] This value is an estimate based on the following reasonings: the differences $\Delta \log \Delta_{M/d(pGpG)/GMP} = \log \Delta_{M/dGMP} - \log \Delta_{M/GMP}$ are for Mg^{2+} 0.07 ± 0.06 [=(0.23 ± 0.05) − (0.16 ± 0.04)], for Zn^{2+} 0.15 ± 0.11 [=(0.84 ± 0.08) − (0.69 ± 0.07)], and for Cu^{2+} 0.17 ± 0.10 [=(1.14 ± 0.07) − (0.97 ± 0.07)]. The corresponding average equals $\Delta \log \Delta = 0.13 \pm 0.09$. Hence, one may transform $\log \Delta_{Cd/GMP} = 0.79 \pm 0.06$ into $\log \Delta_{Cd/dGMP} = (0.79 \pm 0.06) + (0.13 \pm 0.09) = 0.92 \pm 0.11$ as given above.

of a phosphate–phosphate macrochelate upon M^{2+} coordination, $M[d(pGpG)]_{cl/PO}^-$, should be *inhibited* because of the loss of flexibility in the phosphate backbone. This is indeed the case as a comparison of the charge-corrected stability enhancements due to the formation of the 10-membered chelates in $Pb(pUpU)^-$ and $Pb[d(pGpG)]^-$ shows [150,151]: $\log \Delta^*_{Pb/d(pGpG)/cor} - \log \Delta^*_{Pb/pUpU/cor} = (0.79 \pm 0.14) - (1.16 \pm 0.26) = -0.37 \pm 0.30$ (3σ). The absolute value of this *negative* stability difference is in perfect agreement with the *positive* one obtained above, $\Delta \log \Delta^*_{M/d(pGpG)/dGMP/av}$, for Mg^{2+}, Zn^{2+}, and Cd^{2+}. Hence, the summarized observations indicate that some intramolecular purine–purine stacking in $d(pGpG)^{3-}$ occurs, at least in the presence of metal ions.

At first glance, this seems to be in contrast with recent reasonings [149] based on comparisons of the acid–base properties of this dinucleotide in the absence of metal ions: The difference in acidity of the two N1H sites in $d(pGpG)^{3-}$ of $\Delta pK_a = 0.57 \pm 0.16$ (3σ), which is within the error limits identical with the statistically expected value of 0.6 for a symmetrical diprotonic acid [159], let to the conclusion that the two nucleotide units in $d(pGpG)^{3-}$ "react rather independently and do not 'feel' much of each other". In other words, $d(pGpG)^{3-}$ occurs predominately in an open, unstacked form. The larger acidity difference determined for $d(GpG)^-$ ($\Delta pK_{a/N1H} = 1.02 \pm 0.08$) was thereby explained by intramolecular stacking interactions, which are inhibited by the twofold negatively charged 5′-phosphate group in $d(pGpG)^{3-}$ [149]. This comparison of the acid–base properties of $d(pGpG)^{3-}$ and $d(GpG)^-$ now implies that the neutralization of the negative charge by metal ion coordination at the terminal phosphate group restores the stacking abilities of the two guanine nucleobases.

Whether some preorientation of the nucleobase residues already exists within the $d(pGpG)^{3-}$ species or only occurs after metal ion coordination, i.e. formation of the $M[d(pGpG)]_{op}^-$ species (equilibrium (8)), cannot be answered unequivocally because all the differences considered are small and often also close to the error limits [149,151]. Nevertheless, one can estimate the extreme situation of such a preorientation: If the above 0.3 log units (= $\Delta \log \Delta^*_{M/d(pGpG)/dGMP/av}$) would be *completely* due to intramolecular stacking either in $d(pGpG)^{3-}$ and/or in $M[d(pGpG)]_{op}^-$, this would equal a formation degree of 50% for the stacked species (see Table 4, footnote 'd'). On the other hand, a significant amount of this enhancement is certainly due to the "three-point" macrochelation also indicated above which naturally further facilitates the intramolecular stacking interaction. It is thus evident that any preorientation in $d(pGpG)^{3-}$ and in $M[d(pGpG)]_{op}^-$ as well as the interaction of a phosphate-coordinated metal ion with both N7 sites are very much interwoven with each other and hard to separate because they promote each other.

To conclude, if one assumes that only 0.1 or 0.15 log units of the total extra stability enhancement $\Delta \log \Delta^*_{M/d(pGpG)/dGMP/av}$ originates from the intramolecular stack, this corresponds already to formation degrees of the preoriented structure of about 20 or 30%, respectively [158]. Equally important, these formation degrees are connected with only very tiny changes in free energy of $\Delta G^\circ_{(25^\circ C)} = -0.57$ or -0.86 kJ mol^{-1}, respectively [158]. Hence, we are convinced that indeed small but significant amounts of $d(pGpG)^{3-}$, $M[d(pGpG)]_{op}^-$, and even more so of $d(GpG)^-$ [149], exist in the described preorientated stacked form thus facilitating the "three-point" metal ion binding (and/or *vice versa).* It is evident that in larger RNA molecules such preorientations are achieved more easily and that this gives rise to preferred sites for metal ion binding as observed, e.g., with Mg^{2+} in group II introns [21] or the ribosome [19] (see also Section 4.1).

4. Metal ion binding to ribozymes and DNA

Having established and summarized in Section 3 the different metal ion binding properties of mono- and dinucleotides and the structures of their complexes, it will now be interesting to see if parallels can be drawn to existing data of larger nucleic acids. To

the best of our knowledge no detailed structural solution data on the atomic level exist showing the complete binding geometries of metal ions in their binding pockets (perhaps with the exception of DNA quadruplexes [160]) [7]. In the following sections we therefore rely on high resolution solid-state structures of large RNA molecules determined by X-ray crystallography. Because a complete evaluation of the existing structures in the PDB/NDB would go beyond the scope of this review, we concentrate on two types of RNA and one DNA sequence, i.e. the large ribosomal subunit, the HIV-1 dimerization initiation site (DIS), and the so-called Dickerson-Drew DNA dodecamer. Nevertheless, it needs to be emphasized that the conclusions drawn here will hold for all complex RNA structures, as in all instances innersphere and outersphere binding of the metal ions occurs, as e.g. can also be seen in the P4–P5–P6 domains of the *Tetrahymena* group I intron (Fig. 7).

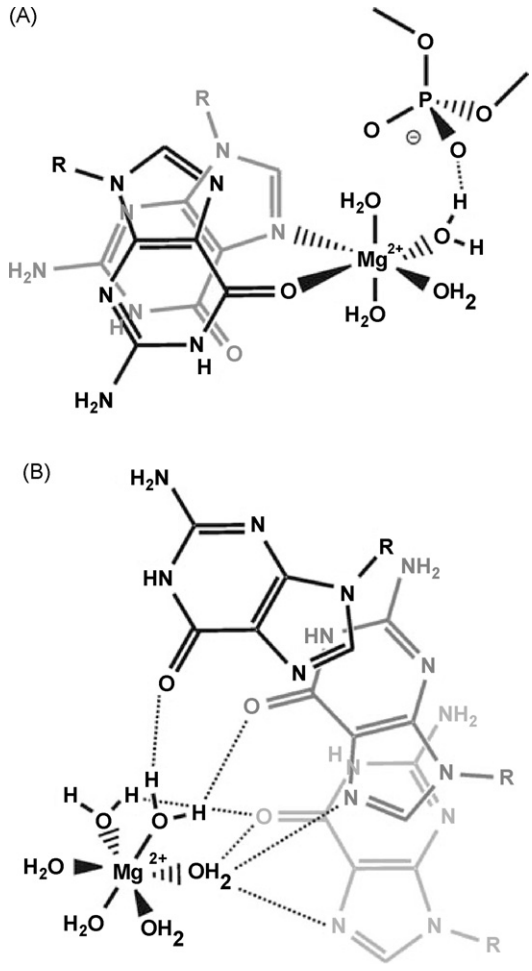

Fig. 7. Innersphere versus outersphere binding of Mg^{2+} (or other metal ions) as it occurs (with mononucleotides or) within larger nucleic acid structures. (A) Binding of Mg^{2+} to one N7 and one carbonyl O6 oxygen of two guanosine residues via innersphere coordination, as well as via a water molecule to a non-bridging phosphate oxygen. The three remaining sites of the hexacoordinated Mg^{2+} are occupied by water molecules (adapted from Ref. [168]). (B) A hexahydrated Mg^{2+} ion is solely bound via water molecules in an outersphere manner to RNA. This figure was adapted from a crystal structure of the P4–P5–P6 domains of the *Tetrahymena* group I intron (PDB 1GID) [5,169].

4.1. Mg^{2+} binding to the ribosome

The ribosomal RNA–protein complex represents the largest nucleic acid structure determined by X-ray crystallography today [2–4]. The large ribosomal subunit of *Haloarcula marismortui* at a resolution of 2.4 Å was additionally analyzed by Klein et al. with respect to its metal ion binding sites [19]. Aside from 88 binding sites for monovalent cations, which will not be discussed here, 116 positions for Mg^{2+} ions have been localized. This ribosome structure therefore represents an ideal basis for investigating the different Mg^{2+} binding modes within a complex RNA architecture.

The 50S subunit of *H. marismortui* comprises 3045 nucleotides (2833 of which could be refined in the crystal structure) [2] and consequently an equal number of negative charges originating from the phosphate groups need to be compensated by metal ions. As the 116 Mg^{2+} and 88 Na^+/K^+ ions identified in the structure add up to 320 positive charges, only 10.6% of the phosphodiester-bridge charges are compensated by these metal ions. Neglecting any further positive charges contributed by the proteins bound, it is obvious that the Mg^{2+} ions identified in the structure represent only the small fraction of divalent metal ions which are relatively tightly bound. Such a more or less tight fixation in a certain coordination environment is a strong indication for site-specific binding.

Out of the 116 Mg^{2+} ions, 30- bridge protein with RNA residues and only two are exclusively bound to protein sites. Considering that the ratio between RNA and proteins in the 50S subunit amounts to 66:34 (w/w), this shows that RNA is obviously the primary target for hard metal ions like Mg^{2+}. Another interesting aspect is that again out of the 116 ions, only nine are bound exclusively by outersphere interactions (Fig. 7B and Fig. 8A)—all others show at least one innersphere coordination and 30 of the Mg^{2+} ions coordinate even directly to three or more sites (Fig. 8). Only one Mg^{2+} seems to be fully dehydrated! From the nine outersphere bound Mg^{2+} ions, three form hydrogen bonds from their first shell water molecules to nucleobase moieties only (Fig. 8A), whereas the other six ions all show contacts to a phosphate oxygen and five of them also to nucleobases or amino acids. Taken together, this is a first indication that the phosphate group is the primary binding site and that contacts to a nucleobase (or phosphate) can be well mediated through outersphere interactions.

As a consequence of the above mentioned numbers in combination with the observation that only five Mg^{2+} ions are coordinated exclusively to nucleobase atoms, two Mg^{2+} ions to proteins and another three only to functional groups of the nucleosides and/or amino acids, the overwhelming majority of the 106 magnesium(II) ions is bound to phosphate groups. The phosphate groups also comprise the majority of innersphere binding sites: from the total of 107 Mg^{2+} ions being coordinated through at least one innersphere contact, 82 (=76.6%) show a minimum of one of these direct contacts to a non-bridging oxygen atom of the phosphate groups (Fig. 8). Out of these 82 ions, 43 Mg^{2+} bridge two or more phosphate groups by innersphere coordination, and another 34 by at least one innersphere and one or more outersphere contacts. Again, the observation that phos-

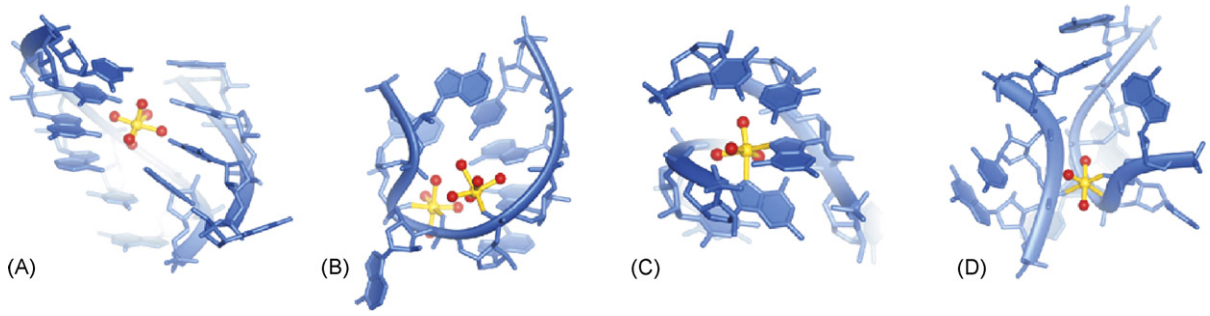

Fig. 8. Mg^{2+} binding in the large ribosomal subunit of *H. marismortui* [19]. (A) A fully hexahydrated Mg^{2+} ion (no. 38, according to the numbering scheme used in Ref. [19]) is located in the major groove and makes solely outersphere contacts to nucleobase functional groups. (B) Two Mg^{2+} ions showing either one (no. 21, in the front) or two (no. 34, in the back) innersphere contacts to non-bridging phosphate-oxygen atoms within a RNA loop structure. In addition, both ions show an extensive network of outersphere contacts, i.e. hydrogen bonds to purine N7 and O6 positions. (C) Shown are two innersphere contacts of a Mg^{2+} (no. 11) in a *cis*-fashion to two guanine N7 positions of two different strands. (D) An extensively dehydrated Mg^{2+} ion (no. 8) bridges two nearby positioned sugar–phosphate backbones via innersphere coordination to three non-bridging phosphate-oxygens. Additional water molecules and further Mg^{2+} and K^+ ions coordinated in the vicinity are omitted for clarity. This figure has been prepared with MOLMOL [167] based on the PDB file 1S72 [19].

phate groups are the primary binding site for Mg^{2+} (and other alkaline earth, divalent 3d-transition as well as Zn^{2+} or Cd^{2+} ions) in nucleic acids is very well in line with the solution studies described in Section 3, and it also shows that Mg^{2+} is bound to phosphate oxygens to a large part (but not exclusively) through innersphere coordination.

The potentiometric pH titrations with mononucleotides show that a metal ion bound to the 5′-terminal phosphate group(s) may undergo additional contacts with the nucleobase, i.e. macrochelates are formed (equilibrium (2)), whose degree of formation is strongly dependent on the kind of metal ion. Can macrochelate formation or simultaneous phosphate–nucleobase coordination also be observed in the ribosome? Considering the 106 phosphate-bound Mg^{2+} cations, the following binding patterns regarding potential macrochelate formation are found:

(i) 21 Mg^{2+} are bound to $–PO_4^-–$ units exclusively (Fig. 8D). This is a surprisingly high number (about 20%) considering the huge amount of alternative binding sites in potentially close proximity to a Mg^{2+} in a complicated architecture like the ribosome.

(ii) 48 Mg^{2+} are bound to at least one phosphate moiety and any one N7 position, corresponding to a "macrochelate-formation" degree of 45% (Figs. 6 as well as 8B and C). Interestingly, 30 of those 48 contacts are actually intra-nucleotide macrochelates, i.e. the phosphate and the N7 position belong to the same nucleotide unit. This corresponds to a formation degree of 28% for intra-nucleotide macrochelates (based on the total 106 Mg^{2+} being bound to phosphate groups), which is extraordinarily close to the one found for the mononucleotide GMP^{2-} (31 ± 7%, see also Table 2) as determined by potentiometric pH titrations [122].

(iii) Out of the 48 Mg^{2+} ions that show a simultaneous phosphate/N7 coordination, 28 exhibit an inter-nucleotide macrochelate between two consecutive nucleotides, thus some Mg^{2+} ions are involved in both intra- and inter-macrochelate formation (Fig. 6). Interestingly, out of these 28 Mg^{2+}, 27 bind to the N7 position of the purine nucleotide that is positioned 3′ to the nucleotide of the coordinated phosphate ($–PO_4^-–_n/N7_{n+1}$), and only four show a bridging of the opposite way, i.e. ($N7_n/–PO_4^-–_{n+1}$). However, this latter binding pattern is actually always part of a *four-fold* coordination involving both phosphate groups and N7 sites, i.e. $–PO_4^-–_n/N7_n/–PO_4^-–_{n+1}/N7_{n+1}$ (Fig. 6). A "three-point" macrochelation as discussed in Section 3.3, also occurs: out of the 28 above mentioned Mg^{2+} ions, 11 show a $–PO_4^-–_n/N7_n/N7_{n+1}$, and 12 ions a $–PO_4^-–_n/–PO_4^-–_{n+1}/N7_{n+1}$ coordination pattern (note that no distinction between outer- and innersphere coordination is made here). The sole coordination patterns $N7_n/–PO_4^-–_{n+1}/N7_{n+1}$ and $–PO_4^-–_n/N7_n/–PO_4^-–_{n+1}$, i.e. without involving the $–PO_4^-–_n$ or $N7_{n+1}$ sites, respectively, do not occur. Propably steric constraints are the reason for this discrimination. However, to investigate and understand the observed discriminations in the various binding patterns, dinucleotides like $d(pGpG)^{3-}$, as discussed in Section 3.2, constitute perfect models, as they allow the exploration of the various patterns in more detail. In fact, the high occurrence of the $–PO_4^-–_n/Z/N7_{n+1}$ Mg^{2+} coordination pattern ($Z = –PO_4^-–_{n+1}$ or $N7_n$) suggests that 5′-PuPu, and 5′-PyPu (but not 5′-PuPy, with Pu = purine and Py = Pyrimidine) sequences are favored metal ion binding motifs in RNAs if one considers matters on the atomic coordination chemical level.

(iv) Besides the N7 position, also the carbonyl O6 of guanines is a potential site for macrochelate formation (Fig. 8B). Indeed, in 19 cases (out of the above-mentioned 30), simultaneous intra-nucleobase coordination to N7 and O6 takes place, whereby in all cases at least one water molecule is involved. There are only five instances where solely O6 (but not N7) is coordinated, but the O6 never belongs to the same nucleotide as the coordinated phosphate oxygen. The same is true for macrochelate formation involving the O4 and O2 positions of pyrimidine bases. In the latter case also no simultaneous coordination to a N7 position of a nearby

purine base can be found. It is also interesting to note that no preference for inner- or outersphere binding to either N7 or carbonyl oxygens can be recognized.

The above listed points based on X-ray crystallographic studies of a large RNA confirm the results from solution studies for Mg^{2+} binding to nucleic acids (Section 3) with a remarkable accuracy: (i) intra-nucleotide macrochelate formation is in the same order, (ii) simultaneous N7 and O6 binding is observed as it has been proposed for nucleotides before [104,122,128], and (iii) no intra-residue coordination to the phosphate group and a carbonyl oxygen of pyrimidine-nucleotide units occurs. To summarize, the structural insight into the ribosome constitutes a very nice example that allows to validate the results from solution studies and to extrapolate even better the data from mononucleotides to larger RNA structures in the future.

4.2. Metal ion binding to the HIV dimerization initiation site

In Section 4.1, the coordination properties of Mg^{2+} ions within a large RNA structure have been analyzed and compared to results from solution studies (Section 3). Keeping in mind the issues raised in the beginning of this review that other metal ions than Mg^{2+} may lead to completely different phenotypical results in terms of ribozyme reactivity, this section now compares the coordinating properties of Mg^{2+}, Ca^{2+}, Mn^{2+}, and Cd^{2+} to a specific RNA sequence.

Ideally, for a comparison of the coordinating properties and geometries of the four mentioned metal ions to RNA, four X-ray structures of identical RNA sequences crystallized with each individual metal ion should be available. We are only aware of one example where this has been accomplished to a certain extent: two related RNA duplexes of the HIV-1 dimerization initiation site (DIS), subtype-A and subtype-B, have been crystallized in the presence of Mg^{2+} and subsequently soaked or co-crystallized with eleven different metal ions (K^+, Ca^{2+}, Sr^{2+}, Ba^{2+}, Mn^{2+}, Co^{2+}, Zn^{2+}, Cd^{2+}, Pb^{2+}, Au^{3+}, Pt^{4+}) [161]. In the present context we will again concentrate on Mg^{2+} in comparison with Ca^{2+}, Mn^{2+}, and Cd^{2+} at the individual binding pockets within these RNAs. However, unfortunately only the pdb files of the Mg^{2+} (PDB IDs 462D and 1Y99) and Mn^{2+} (PDB ID 1Y90) forms are available allowing us a detailed characterization, whereas for Ca^{2+} and Cd^{2+} we can only rely on the content of Ref. [161].

Eight specific Mg^{2+} binding sites were identified in the subtype-A DIS, three of them being identical (α/α′, β/β′, γ/γ′) due to the palindromic sequence, and two being close to each other in the center of the duplex (δ, ε) (see also Fig. 9A). Out of the five unique coordination sites, the coordination sphere of one Mg^{2+} is not refined (ε) but seems to be hexahydrated, and two Mg^{2+} ions (α/α′, β/β′) are fully hexahydrated and bind to the nucleobase functional groups at the major groove edge of GC base pairs only. Two further ions bind near the bulged out adenosine and the adjacent GA base pair (γ/γ′, δ), both of them showing two innersphere contacts. The Mg^{2+} ion in position δ bridges the phosphate groups of the two strands (Fig. 9A and 9C). The γ/γ′-Mg^{2+} site is peculiar because in addition to the two innersphere contacts to a A8-phosphate oxygen and the N7 of guanine 10 it shows four further outersphere contacts (partially bifurcated) to nearby O6, N7 sites as well as to one phosphate oxygen (Fig. 9D). Having the evaluation of the Mg^{2+} binding sites within the ribosome in mind (Section 4.1), it is surprising to see, that in a largely duplex-RNA, the Mg^{2+} ions seem to bind preferably to the functional groups of the nucleotide moieties only in a completely outersphere manner. Only in regions of loops and non-canonical base-pairs innersphere binding and phosphate coordination occurs. The eight Mg^{2+} ions in the HIV–DIS structure described above approximate a charge compensation of 35% of the 46 nucleotide long phosphate–sugar backbone. Interestingly, if one considers only the three partially innersphere bound Mg^{2+} ions (γ/γ′, δ), a charge compensation of only 13% is achieved, which is remarkably similar to the 10.6% found in the ribosome, see Section 4.1). It is left for future studies to see if in the ribosome Mg^{2+} ions bound to the major groove or to regular duplexes were just not detected.

How do the Mg^{2+} binding sites compare with those of Mn^{2+}? Unfortunately the crystal structure of the Mn^{2+} form does not allow a detailed analysis as no water molecules are included in the refinement (PDB ID 1Y90). Nevertheless, all Mg^{2+} positions in the subtype-A DIS can be overlaid pretty well with Mn^{2+} in the crystal structure (Fig. 9B), suggesting that Mn^{2+} indeed is a good replacement for Mg^{2+}. This conclusion is slightly premature, as the Mn^{2+} ions also occupy *additional* sites within this RNA: two more Mn^{2+} ions are found at the terminal base pairs of the helix and another one near one bulged out adenosine. A similar situation is found in the subtype-B duplex, where Mg^{2+} only partially occupies two sites, but Mn^{2+} fully occupies a pocket formed by two phosphates and a guanine N7 [161]. One can therefore conclude the following: first, Mn^{2+} behaves similar to Mg^{2+} in its preference for certain binding sites, which is in accord with the similar extent of macrochelate formation (Tables 2 and 3), and confirmed by the corresponding occupation of distinct sites, and second, Mn^{2+} has a slightly higher affinity towards RNA than Mg^{2+} as the coordination of additional Mn^{2+} ions suggests. Actually the higher affinity towards mono- and dinucleotides already predicted this behavior. Both points are well in line with the relative positioning of Mg^{2+} and Mn^{2+} within the Irving–Williams series and the increasing affinity towards nitrogen ligands when moving further to the right within the 3d series in the Periodic Table [117,123,124].

Ca^{2+} as well as Sr^{2+} and Ba^{2+} are poor mimics of Mg^{2+}, as indicated by the fact that none of these heavier alkaline earth metal ions occupies the same sites as Mg^{2+}. In fact, the coordination sites of Ca^{2+}, Sr^{2+}, and Ba^{2+} are difficult to establish because none is fully occupied. This is actually in line with their larger size, faster ligand exchange rates and lower binding tendencies (Table 1).

Cd^{2+} is very selective in replacing Mg^{2+}. Only at the γ/γ′ site, where a Mg^{2+} ion makes two innersphere contacts with a phosphate oxygen as well as a guanine N7 site, also Cd^{2+} can be localized. No other Mg^{2+} was replaced in the subtype-A structure including the one at the δ position where innersphere

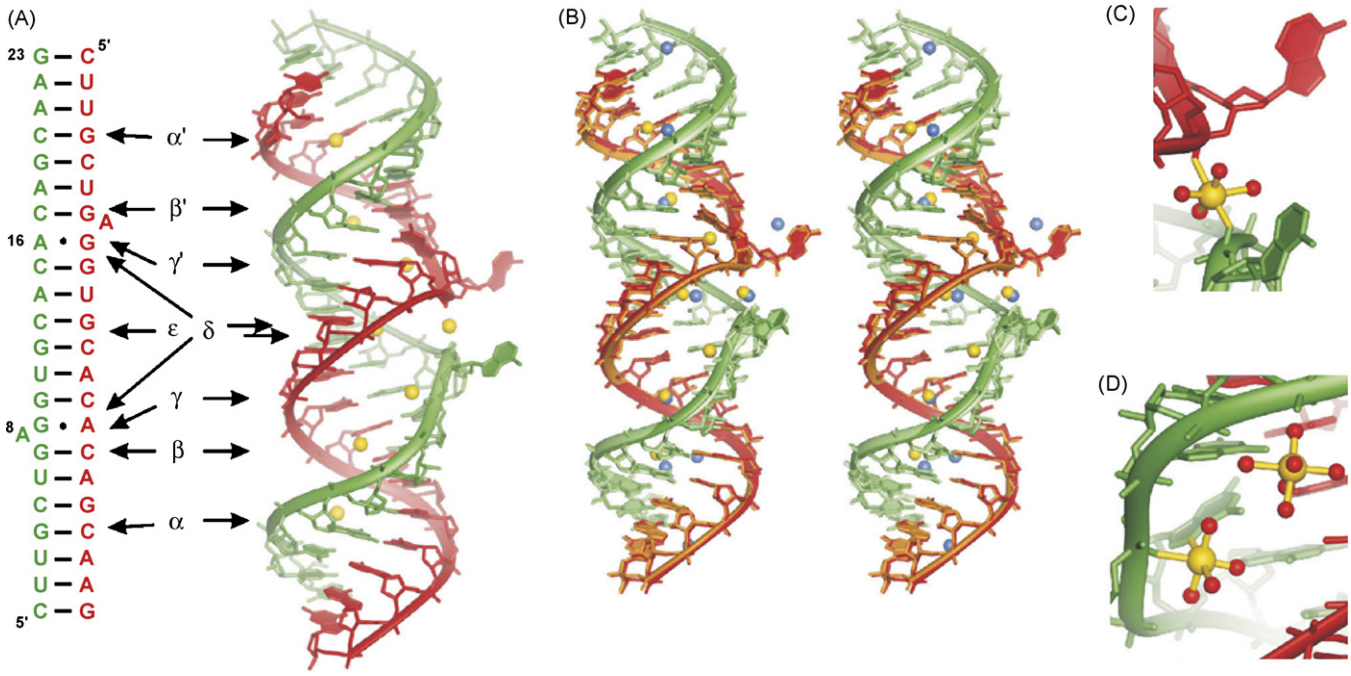

Fig. 9. Metal ion binding to the HIV dimerization initiation site (DIS). (A) The palindromic sequence of the HIV DIS is shown on the left together with its crystal structure to the right, one strand being colored in red and the second one in green. The coordination sites of the Mg^{2+} ions (yellow spheres) are indicated by greek letters. The water molecules have been omitted for clarity. (B) Stereo view of the overlay of the structures of the Mg^{2+} bound (red and dark green) and Mn^{2+} bound (orange and light green) forms. The Mg^{2+} ions are shown as yellow and the Mn^{2+} ions as blue spheres. The water molecules have been omitted for clarity. (C) Close-up view of the δ-coordination site of Mg^{2+} with two innersphere contacts to two non-bridging phosphate-oxygen atoms of A8 and G9 of opposite strands bringing the two backbones close together. All water molecules not being coordinated to Mg^{2+} are omitted for clarity. (D) Close-up view of the ε and γ′-binding sites of Mg^{2+}. The ε-Mg^{2+} is partially dehydrated with two innersphere contacts to the R_P-oxygen of A8 and N7 of G9. All water molecules not being coordinated to the Mg^{2+} ions are omitted for clarity. This figure has been prepared with MOLMOL [167] based on the PDB files 462D (Mg^{2+}) and 1Y90 (Mn^{2+}) [161].

coordination to two phosphates occurs, although Cd^{2+} has a much higher intrinsic affinity towards nucleic acids than Mg^{2+}. This observation illustrates that besides the higher affinity, also the coordinating sites, their geometry and accessibility play an important role: Cd^{2+} seems to be a good replacement for Mg^{2+} only if innersphere coordination to an N7 position (together with possible macrochelate formation) can take place. Again, this corresponds nicely to the results found with mono- and dinucleotides (Section 3) where for Cd^{2+} a high degree of macrochelate formation is found, although one would not have dared to predict that this might be a requirement for Cd^{2+} binding in nucleic acids.

4.3. Metal ion binding to the Dickerson–Drew DNA dodecamer

In the above sections we have seen that RNA can adopt highly complex structures, as e.g. in the ribosome where a large number of the nucleotides are not involved in common Watson–Crick base pairing, but instead in "mismatches", loops, and bulges. As a consequence, complicated three-dimensional architectures are formed with a multitude of (mostly) partly dehydrated Mg^{2+} ions bound within. Evaluation of the Mg^{2+} binding sites within the subtype-A HIV-1 DIS RNA duplex (Section 4.2) showed that partial dehydration of the first coordination sphere seems to occur mainly at unusual, i.e. non-helical, local structures when for example two phosphate–sugar backbones are in close neigh-

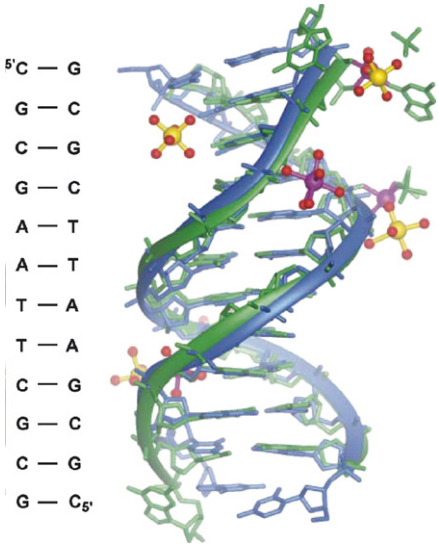

Fig. 10. Mg^{2+} and Ca^{2+} binding to Dickerson–Drew DNA whose sequence is given to the left. The superposition of crystal structures of the Mg^{2+} bound DNA (in blue) and the Ca^{2+} bound form (in green) is shown. It can be clearly seen that the five localized Mg^{2+} ions (yellow spheres, one is on the backside of the duplex) and the four Ca^{2+} ions (magenta spheres) occupy different binding sites. Interestingly, the Mg^{2+} ions are in their hexahydrated form, whereas two of the Ca^{2+} ions undergo partial innersphere coordination to phosphate oxygens and a carbonyl oxygen. The phosphate and the guanine moiety in the top right corner belong to the neighboring DNA duplex, the rest of which has been omitted for clarity. This figure has been prepared with MOLMOL [167] based on the PDB files 436D (Mg^{2+}) [162,163] and 463D (Ca^{2+}) [164].

borhood to each other. It will now be interesting to see, how divalent metal ions are bound to DNA, i.e. a nucleic acid, which adopts majority a regular B-form duplex.

Certainly, the so-called Dickerson–Drew sequence is the structurally best investigated DNA sequence (Fig. 10). However, in terms of binding of divalent metal ions, to the best of our knowledge, there are only structures available in the presence of Mg^{2+} (PDB ID 436D) [162,163] and Ca^{2+} (PDB ID 463D) [164]. The high resolution structure by Egli and co-workers [162,163] reveals three fully occupied and two partially occupied Mg^{2+} sites. Three of the Mg^{2+} ions are in the hexahydrate and two in the pentahydrate form (Fig. 10). The coordination sites of these ions reveal no surprises and are well in-line with the above described findings with mono- and dinucleotides, as well as with the RNAs (Sections 3, 4.1 and 4.2): (i) only one Mg^{2+} is located fully in the major groove whereas all others are found along the phosphate–sugar backbone. These latter ions either bridge two phosphate groups of the same strand, of two strands within the duplex, or of strands of two different DNA duplexes in the crystal lattice. This clearly confirms the phosphate group as being the primary binding site, (ii) the Mg^{2+} located in the major groove is hexahydrated and coordinated solely to the guanine N7 and O6 atoms of two tandem GC base pairs, corresponding nicely to one of the hexahydrated Mg^{2+} ions in the ribosome structure (Fig. 8A and Section 4.1). (iii) The low extent of dehydration is well in line with the observations made with the HIV DIS structure described in Section 4.2, which revealed that dehydration occurs only at places where non-regular structures are present.

The four Ca^{2+} coordination sites coincide in no case with the ones identified for Mg^{2+}, which confirms the results from the HIV DIS RNA evaluation described in Section 4.2. Two Ca^{2+} ions bind in the minor groove, both being heptahydrated and bound to several base functionalities of the DNA only by outer-sphere contacts. The two other Ca^{2+} ions are largely dehydrated and bind along the phosphate–sugar backbone thereby bridging two DNA duplexes in the crystal lattice. These findings confirm that Ca^{2+} indeed is a poor mimic of Mg^{2+}.

Taken together, these two structures of the Dickerson–Drew DNA sequence in presence of Mg^{2+} and Ca^{2+} reveal that in general DNA and RNA behave very similar in terms of their metal ion binding properties.

5. Conclusions and outlook

In this review we have brought together for the first time the extensive knowledge gained from potentiometric pH titrations on metal ion binding of Mg^{2+}, Ca^{2+}, Mn^{2+}, and Cd^{2+} to mono- and dinucleotides in solution, with results available from solid–state studies on large nucleic acid molecules, including the ribosome [19], a HIV dimerization initiation site [161], and the Dickerson–Drew DNA [162–164].

It is amazing to observe how much of the information regarding structures and binding sites can be transferred from the results obtained with low-molecular-weight ligands to the high-molecular-weight nucleic acids. This is very encouraging for the future in a threefold sense: firstly, one may expect that the observations described herein are also valid for other metal ions, e.g. Zn^{2+}. Secondly, the summarized information should help to plan in the future experiments involving metal ions in a more sophisticated way than in the past. Thirdly, one may use the knowledge summarized in this review to make predictions, based on the known coordination chemistry of nucleotides, towards the metal ion-binding properties of RNAs and DNAs in general.

Acknowledgements

The support of our studies by the University of Zürich and the Swiss National Science Foundation is gratefully acknowledged: SNF grant 21-105269/1 to E.F. and SNF-Förderungsprofessur to RKOS, PP002-68733/1.

References

[1] R.F. Gesteland, T.R. Cech, J.F. Atkins (Eds.), The RNA World, 3rd ed., Cold Spring Harbor Press, 2006.
[2] N. Ban, P. Nissen, J. Hansen, P.B. Moore, T.A. Steitz, Science 289 (2000) 902.
[3] F. Schlünzen, A. Tocilj, R. Zarivach, J. Harms, M. Gluehmann, D. Janell, A. Bashan, H. Bartels, I. Agmon, F. Franceschi, A. Yonath, Cell 102 (2000) 615.
[4] B.T. Wimberly, D.E. Brodersen, W.M. Clemons Jr., R.J. Morgan-Warren, A.P. Carter, C. Vonrhein, T. Hartsch, V. Ramakrishnan, Nature 407 (2000) 327.
[5] J.H. Cate, R.L. Hanna, J.A. Doudna, Nat. Struct. Biol. 4 (1997) 553.
[6] C.C. Correll, B. Freeborn, P.B. Moore, J.A. Steitz, Cell 91 (1997) 705.
[7] R.K.O. Sigel, A.M. Pyle, Chem. Rev. 107 (2007) 97.
[8] R.K.O. Sigel, Eur. J. Inorg. Chem. 12 (2005) 2281.
[9] R. Shiman, D.E. Draper, J. Mol. Biol. 302 (2000) 79.
[10] G.S. Manning, Biophys. Chem. 7 (1977) 141.
[11] D.E. Draper, D. Grilley, A.M. Soto, Annu. Rev. Biophys. Biomol. Struct. 34 (2005) 221.
[12] V.K. Misra, D.E. Draper, J. Mol. Biol. 317 (2002) 507.
[13] V.K. Misra, D.E. Draper, Proc. Natl. Acad. Sci. U.S.A. 98 (2001) 12456.
[14] V.K. Misra, D.E. Draper, Biopolymers 48 (1998) 113.
[15] G.S. Manning, Quart. Rev. Biophys. 11 (1978) 179.
[16] G.S. Manning, Biopolymers 69 (2003) 137.
[17] C.F. Anderson, M.T. Record Jr., Annu. Rev. Biophys. Biophys. Chem. 19 (1990) 423.
[18] C.F. Anderson, M.T. Record Jr., Biophys. Chem. 11 (1980) 353.
[19] D.J. Klein, P.B. Moore, T.A. Steitz, RNA 10 (2004) 1366.
[20] S. Dorner, A. Barta, Biol. Chem. 380 (1999) 243.
[21] R.K.O. Sigel, A. Vaidya, A.M. Pyle, Nat. Struct. Biol. 7 (2000) 1111.
[22] C. Berens, B. Streicher, R. Schroeder, W. Hillen, Chem. Biol. 5 (1998) 163.
[23] A.M. Pyle, Met. Ions Biol. Syst. 32 (1996) 479.
[24] V.J. DeRose, Curr. Opin. Struct. Biol. 13 (2003) 317.
[25] A.M. Pyle, J. Biol. Inorg. Chem. 7 (2002) 679.
[26] M.J. Fedor, Curr. Opin. Struct. Biol. 12 (2002) 289.
[27] L.D. Williams, Top. Curr. Chem. 253 (2005) 77.
[28] R.K.O. Sigel, A.M. Pyle, Met. Ions Biol. Syst. 40 (2003) 477.
[29] B. Knobloch, M.C. Erat, R.K.O. Sigel, in preparation.
[30] M.C. Erat, O. Zerbe, T. Fox, R.K.O. Sigel, ChemBioChem 8 (2007) 306.
[31] M.C. Erat, R.K.O. Sigel, submitted for publication.
[32] B. Knobloch, R.K.O. Sigel, Chimia 60 (2006) 408.
[33] R.L. Gonzalez Jr., I. Tinoco Jr., J. Mol. Biol. 289 (1999) 1267.
[34] T.C. Gluick, R.B. Gerstner, D.E. Draper, J. Mol. Biol. 270 (1997) 451.
[35] J.H. Davis, M. Tonelli, L.G. Scott, L. Jaeger, J.R. Williamson, S.E. Butcher, J. Mol. Biol. 351 (2005) 371.
[36] R.K.O. Sigel, D.G. Sashital, D.L. Abramovitz, A.G. Palmer III, S.E. Butcher, A.M. Pyle, Nat. Struct. Mol. Biol. 11 (2004) 187.
[37] A. Vaidya, H. Suga, Biochemistry 40 (2001) 7200.
[38] M. Hertweck, M.W. Müller, Eur. J. Biochem. 268 (2001) 4610.

[39] S.R. Morrissey, T.E. Horton, V.J. DeRose, J. Am. Chem. Soc. 122 (2000) 3473.
[40] T.E. Horton, D.R. Clardy, V.J. DeRose, Biochemistry 37 (1998) 18094.
[41] Y. Tanaka, K. Taira, Rec. Res. Dev. Org. Chem. 9 (2005) 93.
[42] Y. Tanaka, K. Taira, Chem. Commun. (2005) 2069.
[43] B. Knobloch, R.K.O. Sigel, in preparation.
[44] I. Bertini, A. Sigel, H. Sigel (Eds.), Handbook on Metalloproteins, Marcel Dekker Inc., New York, 2001.
[45] E.M. Osborne, J.E. Schaak, V.J. DeRose, RNA 11 (2005) 187.
[46] M. Roychowdhury-Saha, D.H. Burke, RNA 12 (2006) 1846.
[47] A.S. Burton, N. Lehman, Biochimie 88 (2006) 819.
[48] M.C. Erat, O. Fedorova, R.K.O. Sigel, in preparation.
[49] A.K. Brown, J. Li, C.M.B. Pavot, Y. Lu, Biochemistry 42 (2003) 7152.
[50] Y. Lu, J. Liu, J. Li, P.J. Bruesehoff, C.M.B. Pavot, A.K. Brown, Biosens. Bioelectron. 18 (2003) 529.
[51] Y. Lu, Chem. Eur. J. 8 (2002) 4588.
[52] M.C. Erat, M. Wächter, R.K.O. Sigel, CHIMIA 58 (2004) 479.
[53] M.J. Berridge, Biochim. Biophys. Acta 1742 (2004) 3.
[54] G. Ermak, K.J.A. Davies, Mol. Immunol. 38 (2001) 713.
[55] T. Pozzan, R. Rizzuto, Nat. Cell Biol. 2 (2000) E25–E27.
[56] R.G. Hansford, D. Zorov, Mol. Cell. Biochem. 184 (1998) 359.
[57] E. Carafoli, Nat. Rev. Mol. Cell Biol. 4 (2003) 326.
[58] E. Carafoli, Trends Biochem. Sci. 28 (2003) 175.
[59] R.L. Gonzalez Jr., I. Tinoco Jr., Methods Enzymol. 338 (2001) 421.
[60] P.M. Gordon, J.A. Piccirilli, Nat. Struct. Biol. 8 (2001) 893.
[61] S.-O. Shan, A.V. Kravchuk, J.A. Piccirilli, D. Herschlag, Biochemistry 40 (2001) 5161.
[62] M.P. Latham, D.J. Brown, S.A. McCallum, A. Pardi, ChemBioChem 6 (2005) 1492.
[63] K.F. Blount, O.C. Uhlenbeck, Annu. Rev. Biophys. Biomol. Struct. 34 (2005) 415.
[64] J. Hsieh, C.A. Fierke, Encycl. Biol. Chem. 3 (2004) 733.
[65] C. Hammann, D.M.J. Lilley, ChemBioChem 3 (2002) 690.
[66] S.E. Butcher, Curr. Opin. Struct. Biol. 11 (2001) 315.
[67] J.B. Murray, A.A. Seyhan, N.G. Walter, J.M. Burke, W.G. Scott, Chem. Biol. 5 (1998) 587.
[68] J.L. O'Rear, S. Wang, A.L. Feig, L. Beigelman, O.C. Uhlenbeck, D. Herschlag, RNA 7 (2001) 537.
[69] M. Martick, W.G. Scott, Cell 126 (2006) 309.
[70] A.L. Feig, W.G. Scott, O.C. Uhlenbeck, Science 279 (1998) 81.
[71] J.B. Murray, D.P. Terwey, L. Maloney, A. Karpeisky, N. Usman, L. Beigelman, W.G. Scott, Cell 92 (1998) 665.
[72] S. Wang, K. Karbstein, A. Peracchi, L. Beigelman, D. Herschlag, Biochemistry 38 (1999) 14363.
[73] M. Maderia, L.M. Hunsicker, V.J. DeRose, Biochemistry 39 (2000) 12113.
[74] M.D. Canny, F.M. Jucker, E. Kellogg, A. Khvorova, S.D. Jayasena, A. Pardi, J. Am. Chem. Soc. 126 (2004) 10848.
[75] M. De la Pena, S. Gago, R. Flores, EMBO J. 22 (2003) 5561.
[76] A. Khvorova, A. Lescoute, E. Westhof, S.D. Jayasena, Nat. Struct. Biol. 10 (2003) 708.
[77] K. Lehmann, U. Schmidt, Crit. Rev. Biochem. Mol. Biol. 38 (2003) 249.
[78] A.M. Pyle, Science 261 (1993) 709.
[79] P.Z. Qin, A.M. Pyle, Biochemistry 36 (1997) 4718.
[80] L.J. Su, C. Waldsich, A.M. Pyle, Nucleic Acids Res. 33 (2005) 6674.
[81] P.M. Gordon, E.J. Sontheimer, J.A. Piccirilli, RNA 6 (2000) 199.
[82] P.M. Gordon, E.J. Sontheimer, J.A. Piccirilli, Biochemistry 39 (2000) 12939.
[83] E.J. Sontheimer, P.M. Gordon, J.A. Piccirilli, Genes Dev. 13 (1999) 1729.
[84] M. Boudvillain, A.M. Pyle, EMBO J. 17 (1998) 7091.
[85] M. Boudvillain, A. de Lencastre, A.M. Pyle, Nature 406 (2000) 315.
[86] N. Lehman, G.F. Joyce, Curr. Biol. 3 (1993) 723.
[87] N. Lehman, G.F. Joyce, Nature 361 (1993) 182.
[88] P.L. Adams, M.R. Stahley, A.B. Kosek, J. Wang, S.A. Strobel, Nature 430 (2004) 45.
[89] M.R. Stahley, S.A. Strobel, Science 309 (2005) 1587.
[90] J. Li, W.C. Zheng, A.H. Kwon, Y. Lu, Nucleic Acids Res. 28 (2000) 481.
[91] S.W. Santoro, G.F. Joyce, Proc. Natl. Acad. Sci. U.S.A. 94 (1997) 4262.
[92] D. Faulhammer, M. Famulok, Angew. Chem., Int. Ed. 35 (1996) 2837.
[93] D. Faulhammer, M. Famulok, J. Mol. Biol. 269 (1997) 188.
[94] A. Peracchi, J. Biol. Chem. 275 (2000) 11693.
[95] S.W. Santoro, G.F. Joyce, Biochemistry 37 (1998) 13330.
[96] J. Li, Y. Lu, J. Am. Chem. Soc. 122 (2000) 10466.
[97] J.W. Liu, Y. Lu, Chem. Mater. 16 (2004) 3231.
[98] J.W. Liu, Y. Lu, J. Fluoresc. 14 (2004) 343.
[99] J.W. Liu, Y. Lu, Anal. Chem. 75 (2003) 6666.
[100] Y. Lu, J.W. Liu, J. Li, P.J. Bruesehoff, C.M.B. Pavot, A.K. Brown, Biosens. Bioelectron. 18 (2003) 529.
[101] H.C. Losey, A.J. Ruthenburg, G.L. Verdine, Nat. Struct. Mol. Biol. 13 (2006) 153.
[102] G.C. Ireton, M.E. Black, B.L. Stoddard, Structure 11 (2003) 961.
[103] M. Kolberg, K.R. Strand, P. Graff, K.K. Andersson, Biochim. Biophys. Acta 1699 (2004) 1.
[104] H. Sigel, R. Griesser, Chem. Soc. Rev. 34 (2005) 875.
[105] H. Sigel, Coord. Chem. Rev. 100 (1990) 453.
[106] T.A. Steitz, J.A. Steitz, Proc. Natl. Acad. Sci. U.S.A. 90 (1993) 6498.
[107] E. Freisinger, A.P. Grollman, H. Miller, C. Kisker, EMBO J. 23 (2004) 1494.
[108] Y.W. Yin, T.A. Steitz, Cell 116 (2004) 393.
[109] T.A. Steitz, Curr. Opin. Struct. Biol. 14 (2004) 4.
[110] L.W. Tari, A. Matte, H. Goldie, L.T.J. Delbaere, Nat. Struct. Biol. 4 (1997) 990.
[111] I. Sagi, Y. Hochman, G. Bunker, S. Carmeli, C. Carmeli, J. Synchr. Rad. 6 (1999) 409.
[112] H. Sigel, Inorg. Chim. Acta 198-200 (1992) 1.
[113] H. Sigel, Eur. J. Biochem. 165 (1987) 65.
[114] H. Sigel, E.M. Bianchi, N.A. Corfu, Y. Kinjo, R. Tribolet, R.B. Martin, J. Chem. Soc., Perkin Trans. 2 (2001) 507.
[115] H. Sigel, Pure Appl. Chem. 76 (2004) 375.
[116] H. Sigel, R. Tribolet, R. Malini-Balakrishnan, R.B. Martin, Inorg. Chem. 26 (1987) 2149.
[117] R.K.O. Sigel, H. Sigel, Met. Ions Life Sci. 2 (2007) 109.
[118] E.M. Bianchi, S.A.A. Sajadi, B. Song, H. Sigel, Chem. Eur. J. 9 (2003) 881.
[119] H. Sigel, S.S. Massoud, R. Tribolet, J. Am. Chem. Soc. 110 (1988) 6857.
[120] R.K.O. Sigel, B. Song, H. Sigel, J. Am. Chem. Soc. 119 (1997) 744.
[121] R.B. Martin, H. Sigel, Comments Inorg. Chem. 6 (1988) 285.
[122] H. Sigel, B. Song, Met. Ions Biol. Syst. 32 (1996) 135.
[123] H. Irving, R.J.P. Williams, Nature 162 (1948) 746.
[124] H. Irving, R.J.P. Williams, J. Chem. Soc. (1953) 3192.
[125] R.B. Martin, Met. Ions Biol. Syst. 20 (1986) 21.
[126] R.B. Martin, in: R.B. King (Ed.), Encyclopedia of Inorganic Chemistry, vol. 4, Wiley, Chichester, 1994, p. 2185.
[127] R.B. Martin, in: R.A. Meyers (Ed.), Encyclopedia of Molecular Biology and Molecular Medicine, vol. 1, VCH, Weinheim, 1996, p. 125.
[128] H. Sigel, S.S. Massoud, N.A. Corfù, J. Am. Chem. Soc. 116 (1994) 2958.
[129] K. Aoki, Acta Crystallogr. B 32 (1976) 1454.
[130] L.E. Kapinos, A. Holý, J. Günter, H. Sigel, Inorg. Chem. 40 (2001) 2500.
[131] G. Kampf, L.E. Kapinos, R. Griesser, B. Lippert, H. Sigel, J. Chem. Soc. Perkin Trans. 2 (2002) 1320.
[132] K. Aoki, Met. Ions Biol. Syst. 32 (1996) 91.
[133] K. Aoki, in: M. Vaghefi (Ed.), Nucleoside Triphosphates and Their Analogs, Taylor & Francis, Boca Raton, USA, 2005, p. 115.
[134] J.K. Shiba, R. Bau, Inorg. Chem. 17 (1978) 3484.
[135] K. Aoki, W. Saenger, J. Inorg. Biochem. 20 (1984) 225.
[136] G.R. Clark, J.D. Orbell, Acta Crystallogr. B 34 (1978) 1815.
[137] K. Aoki, J. Chem. Soc., Chem. Commun. (1979) 589.
[138] K. Aoki, W. Saenger, J. Chem. Soc., Dalton Trans. (1984) 1401.
[139] K. Trueblood, P. Horn, V. Luzzati, Acta Crystallogr. 14 (1961) 965.
[140] T. Sato, Acta Crystallogr. C 40 (1984) 736.
[141] B. Knobloch, W. Linert, H. Sigel, Proc. Natl. Acad. Sci. U.S.A. 102 (2005) 7459.
[142] B. Knobloch, H. Sigel, J. Biol. Inorg. Chem. 9 (2004) 365.
[143] P. De Meester, D.M. Goodgame, T.J. Jones, A.C. Skapski, Biochem. J. 139 (1974) 791.

[144] M.V. Capparelli, D.M.L. Goodgame, P.B. Hayman, A.C. Skapski, Inorg. Chim. Acta 125 (1986) L47.
[145] R. Cini, M. Sabat, M. Sundaralingam, M.C. Burla, A. Nunzi, G. Polidori, P.F. Zanazzi, J. Biomol. Struct. Dyn. 1 (1983) 633.
[146] R. Cini, M.C. Burla, A. Nunzi, G.P. Polidori, P.F. Zanazzi, J. Chem. Soc., Dalton Trans. (1984) 2467.
[147] R. Cini, L.G. Marzilli, Inorg. Chem. 27 (1988) 1855.
[148] M. Sabat, R. Cini, T. Haromy, M. Sundaralingam, Biochemistry 24 (1985) 7827.
[149] B. Knobloch, H. Sigel, A. Okruszek, R.K.O. Sigel, Org. Biomol. Chem. 4 (2006) 1085.
[150] B. Knobloch, D. Suliga, A. Okruszek, R.K.O. Sigel, Chem. Eur. J. 11 (2005) 4163.
[151] B. Knobloch, H. Sigel, A. Okruszek, R.K.O. Sigel, Chem. Eur. J. 13 (2007) 306.
[152] B. Song, H. Sigel, Inorg. Chem. 37 (1998) 2066.
[153] H. Sigel, C.P. Da Costa, R.B. Martin, Coord. Chem. Rev. 219–221 (2001) 435.
[154] K.H. Scheller, F. Hofstetter, P.R. Mitchell, B. Prijs, H. Sigel, J. Am. Chem. Soc. 103 (1981) 247.
[155] O. Yamauchi, A. Odani, H. Masuda, H. Sigel, Met. Ions Biol. Syst. 32 (1996) 207.
[156] P.R. Mitchell, H. Sigel, Eur. J. Biochem. 88 (1978) 149.
[157] H. Sigel, Pure Appl. Chem. 70 (1998) 969.
[158] H. Sigel, L.E. Kapinos, Coord. Chem. Rev. 200-202 (2000) 563.
[159] H. Sigel, B. Lippert, Pure Appl. Chem. 70 (1998) 845.
[160] A. Wong, G. Wu, J. Am. Chem. Soc. 125 (2003) 13895.
[161] E. Ennifar, P. Walter, P. Dumas, Nucleic Acids Res. 31 (2003) 2671.
[162] V. Tereshko, G. Minasov, M. Egli, J. Am. Chem. Soc. 121 (1999) 470.
[163] V. Tereshko, G. Minasov, M. Egli, J. Am. Chem. Soc. 121 (1999) 6970.
[164] J. Liu, J.A. Subirana, J. Biol. Chem. 274 (1999) 24749.
[165] H. Sigel, E.M. Bianchi, N.A. Corfú, Y. Kinjo, R. Tribolet, R.B. Martin, Chem. Eur. J. 7 (2001) 3729.
[166] H. Sigel, D.B. McCormick, Accounts Chem. Res. 3 (1970) 201.
[167] R. Koradi, M. Billeter, K. Wüthrich, J. Mol. Graphics 14 (1996) 51.
[168] I. Tinoco Jr., J.S. Kieft, Nat. Struct. Biol. 4 (1997) 509.
[169] J.H. Cate, A.R. Gooding, E. Podell, K. Zhou, B.L. Golden, C.E. Kundrot, T.R. Cech, J.A. Doudna, Science 273 (1996) 1678.
[170] R.D. Shannon, Acta Crystallogr. A 32 (1976) 751.
[171] W.E. Morf, W. Simon, Helv. Chim. Acta 54 (1971) 794.
[172] C.F. Baes Jr., R.E. Mesmer (Eds.), The Hydrolysis of Cations, Krieger Publishing Co., Malabar, FL, 1976.
[173] L. Helm, A.E. Merbach, Coord. Chem. Rev. 187 (1999) 151.
[174] S.F. Lincoln, Helv. Chim. Acta 88 (2005) 523.
[175] Y. Inada, A.M. Mohammed, H.H. Loeffler, S. Funahashi, Helv. Chim. Acta 88 (2005) 461.
[176] E.M. Bianchi, Ph.D. Thesis, University of Basel, Logos Verlag, Berlin, Switzerland, 2003.